

## Supplementary Information

### A Robust Two-Dimensional Hydrogen-Bonded Network for the Predictable Assembly of Ternary Co-crystals.

*Vijay Srirambhatla<sup>a</sup>, Arno Kraft<sup>a</sup>, Stephen Watt<sup>b</sup>, Anthony V Powell<sup>c</sup>\**

<sup>a</sup>Institute of Chemical Sciences, School of Engineering and Physical Sciences, Heriot-Watt University, Edinburgh EH14 4AS, UK.

<sup>b</sup>Solid Form Solutions Ltd, 1, The Fleming Building, Edinburgh Technopole, Milton Bridge, Nr. Penicuik, EH26 0BE, UK.

Department of Chemistry, University of Reading, Whiteknights, Reading RG6 6AD, UK. E-mail: a.v.powell@reading.ac.uk; Fax: +44 118 378 6331. Tel:+44 118 378 6585

#### Contents:

1. Experimental details of co-crystals **(1) – (10)**.
2. Crystallization experiments involving co-crystals **(1) – (3)** and **(8) – (10)**.
3. ORTEP and packing diagrams of co-crystals **(1) – (3)**, **(8) – (10)**.
4. Powder pattern fitting for co-crystals **(4) - (7)** and resulting unit cell parameters
5. Crystallographic data and geometric parameters for co-crystals **(1) – (3)**, **(8) – (10)**.
6. Thermal analysis data for co-crystals **(1) – (3)**, **(8) – (10)**.
7. Spectroscopic data for co-crystals **(1) – (3)**, **(8) – (10)**.
8. Comparison of bulk powder X-ray diffraction data of ternary co-crystals **(2)**, **(3)**, **(8) – (10)** with respective single crystal simulated powder X-ray patterns

## 1. Experimental details of co-crystals (1) – (10)

### Mechanochemical synthesis of co-crystal (1):

All starting materials were obtained from Aldrich and were used as such without further purification. Furosemide (330 mg, 1.00 mmol) and 4,4'-bipyridyl (78 mg, 0.5 mmol) were ground together for 4–5 min in the presence of 40  $\mu$ l of acetonitrile using a mortar and pestle.

### Co-crystal synthesis of furosemide : bipyridyl at 1-1 composition.

Furosemide (330 mg, 1.00 mmol) and 4,4'-bipyridyl (156 mg, 1.0 mmol) were ground together for 4–5 min in the presence of 40  $\mu$ l of acetonitrile using a mortar and pestle. The co-crystallization at 1-1 composition of furosemide and 4,4'-bipyridyl resulted in the formation of physical mixture as shown in the powder X-ray diffraction comparison plot below (Figure S1).

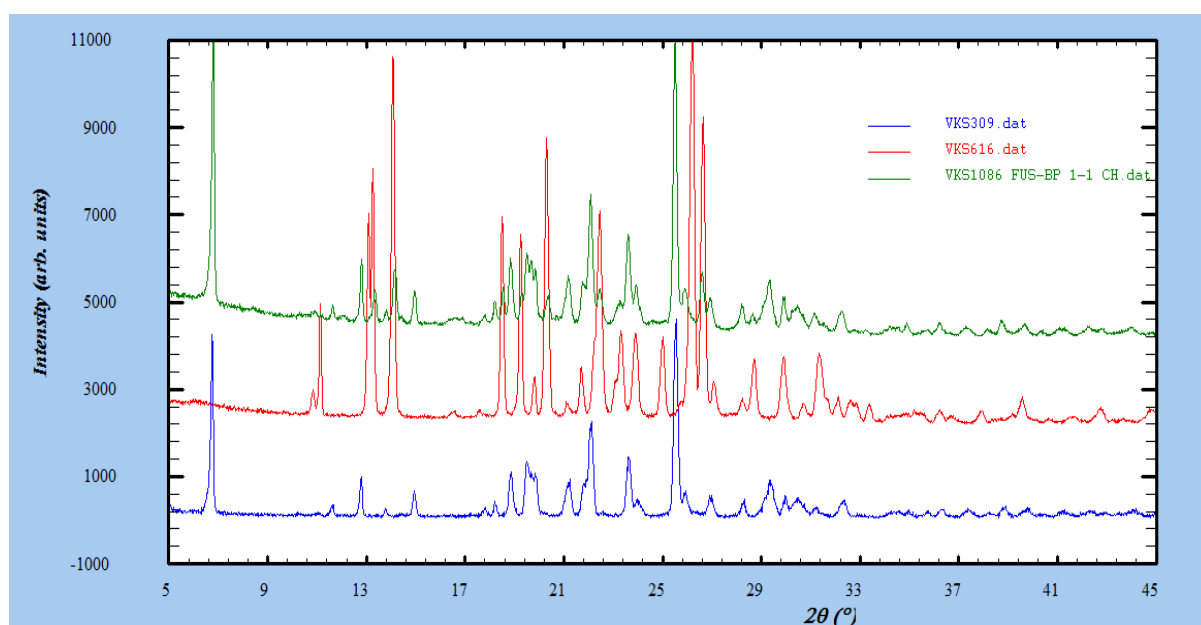


**Figure S1:** Powder diffraction pattern showing the physical mixture between furosemide and bipyridyl at 1:1 composition. (Key: blue- powder pattern of furosemide (fus), red- powder pattern of 4,4'-bipyridyl (bipy), green-powder pattern of mechanochemically synthesised co-crystals of fus:bipy at 1:1 composition).

### Mechanochemical synthesis of co-crystal (2) - (9):

Furosemide (330 mg, 1.00 mmol) and 4,4'-bipyridyl (156 mg, 1.00 mmol) together were grinded in the presence of 20  $\mu$ l of dimethyl sulphoxide (DMSO), methanol, dimethylformamide, ethanol, 2-propanol, 1-butanol, ethylene glycol or 1,4-butanediol to synthesize co-crystals (2) – (9), respectively, in a mortar and pestle for 4-5 min.

### Mechanochemical synthesis of co-crystal (10).

Furosemide (330 mg, 1.00 mmol), bipyridyl (156 mg, 1.00 mmol) and hydroquinone (5.5 mg, 0.5 mmol) were grinded together with 20  $\mu$ l of acetonitrile.

The resulting powders obtained from solvent drop grinding methods were analysed by powder X-ray diffraction.

### 2. Crystallization experiments involving co-crystals (1) – (3) and (8) – (10).

Single crystals of (1) were obtained by slow crystallisation of furosemide (330 mg, 1.00 mmol) and 4,4'-bipyridyl (78 mg, 0.5 mmol) from acetonitrile.

Single crystals of (2), (3), (8), (9) were obtained by dissolving the polycrystalline material obtained from solvent drop grinding in dimethyl sulphoxide (DMSO), methanol, ethylene glycol and 1,4-butanediol. Single crystals of co-crystals of (2), (3), (8) and (9) were isolated after 5 days from the respective crystallization flasks.

Single crystals of (10) were obtained after 4 days by dissolving the molar amounts of furosemide (330 mg, 1.00 mmol), 4,4'-bipyridyl (156 mg, 1.00 mmol), hydroquinone (5.5 mg, 0.5 mmol) in acetonitrile.

### 3. ORTEP and packing diagrams of co-crystals (1) – (3), (8) – (10).

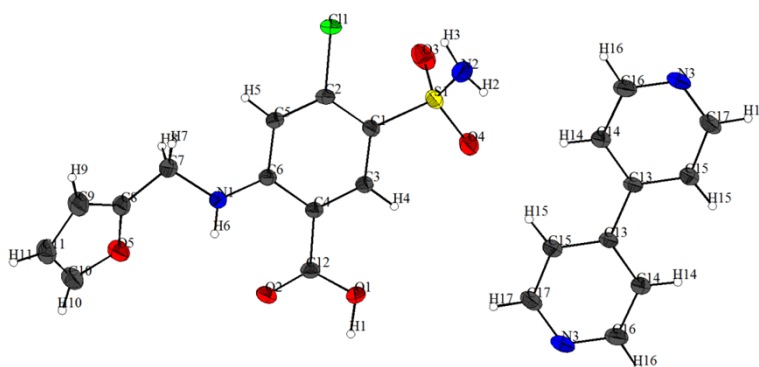


**Figure S2:** ORTEP picture of co-crystal (1) (furosemide – bipyridyl) (1: 0.5). (Key: Sulphur - yellow; chlorine - green; nitrogen - blue; oxygen - red; carbon - grey; hydrogen - white).

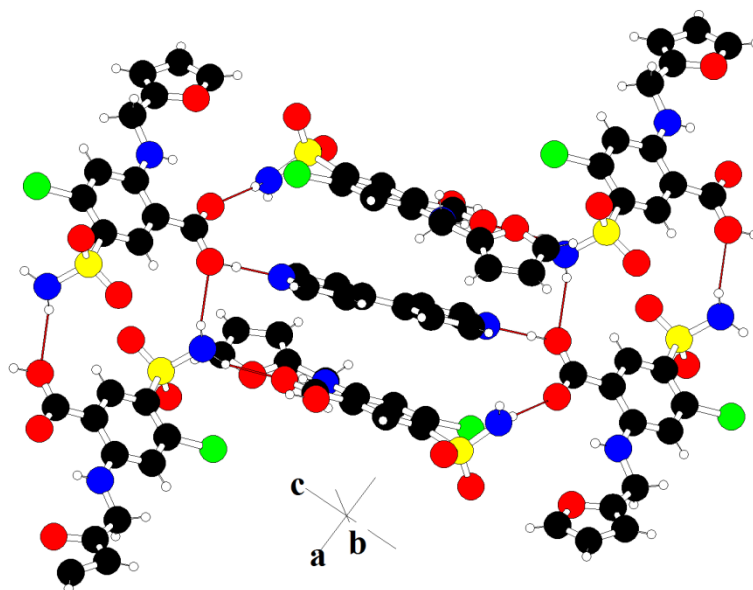


**Figure S3:** Packing arrangement of co-crystal (1) (furosemide – bipyridyl) (1:0.5), with the solid red lines representing the intermolecular hydrogen bonding interactions. (Key: Sulphur -yellow circles; chlorine - green circles; nitrogen - blue circles; oxygen - red circles; carbon - black circles; hydrogen - small white circles).

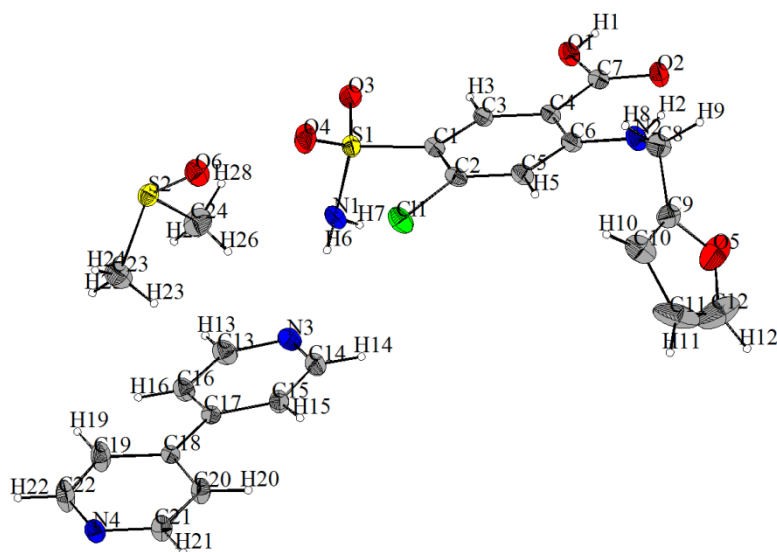


**Figure S4:** ORTEP picture of Co-crystal (2) (furosemide– bipyridyl – DMSO) (1:1:1). (Key: as for Figure S2)

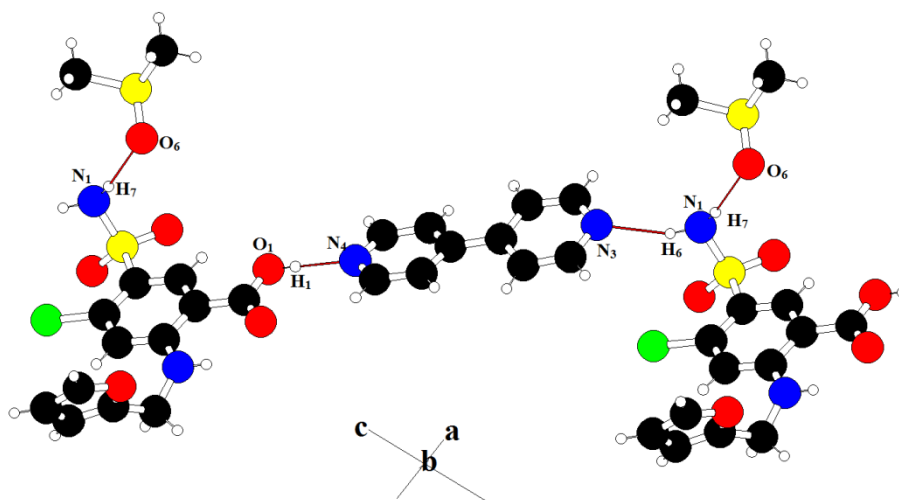


**Figure S5:** Packing arrangement in co-crystal (**2**) (furosemide – bipyridyl – DMSO) in [010] direction. (Key: as for Figure S3)

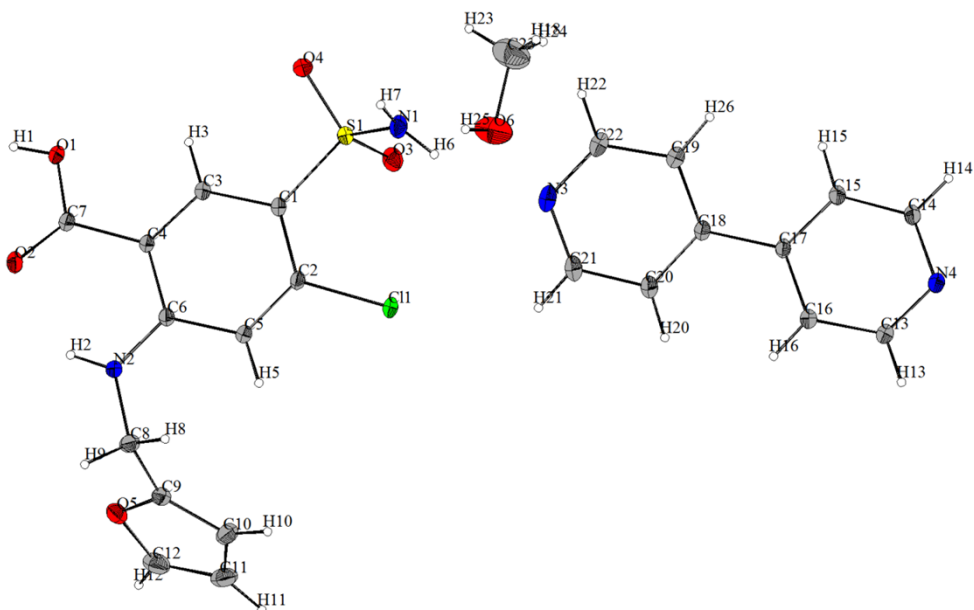


**Figure S6:** ORTEP picture of co-crystal (**3**) (furosemide – bipyridyl – MeOH) (1:1:1). (Key: as for Figure S2)

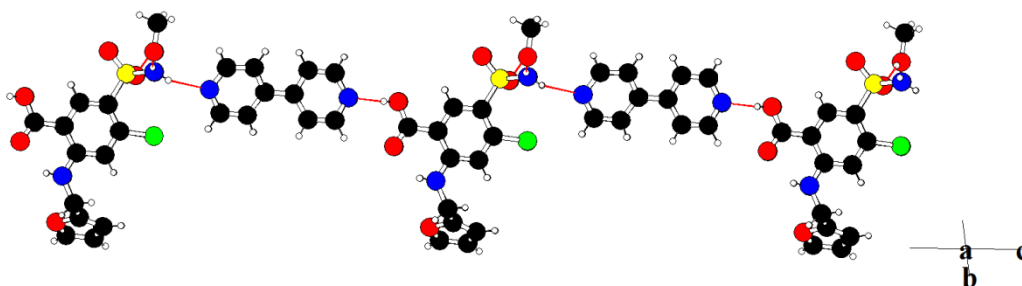


**Figure S7:** Packing arrangement in co-crystal (**3**) (furosemide – bipyridyl – MeOH) in [100] direction. (Key: as for Figure S3)

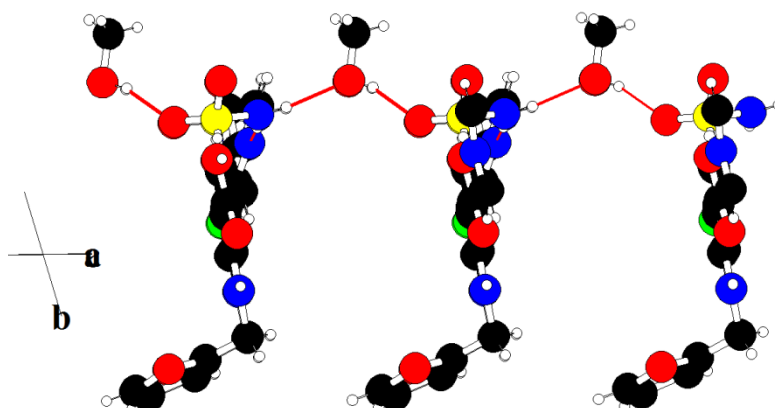


**Figure S8:** Packing arrangement representing the interactions between fus-bipy aggregates and ternary component methanol in co-crystal (**3**) (furosemide – bipyridyl – MeOH). (Key: as for Figure S3)

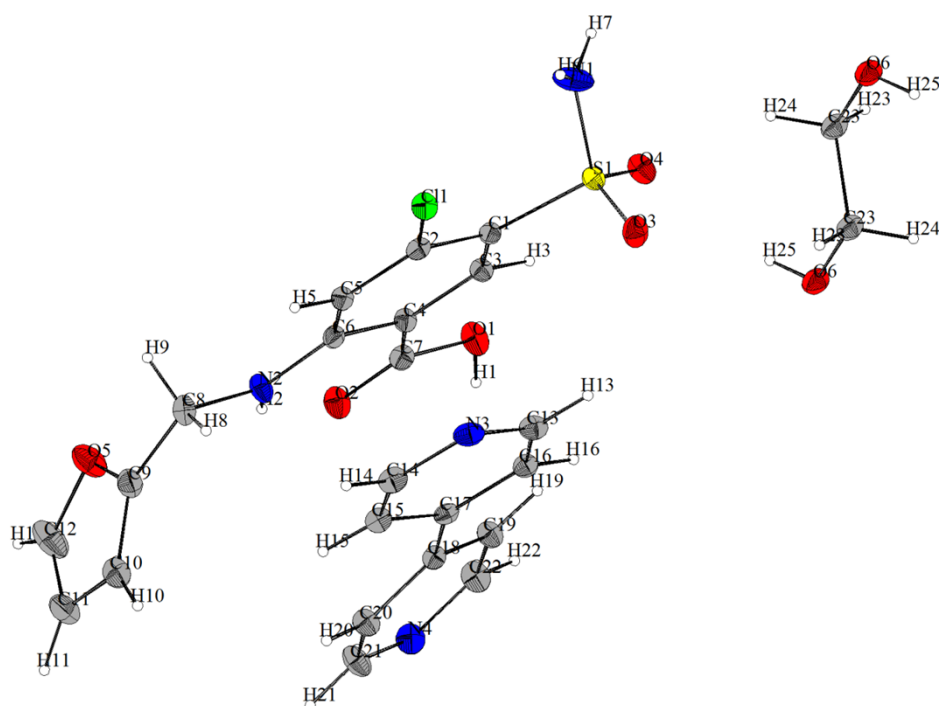


**Figure S9:** ORTEP picture of co-crystal (**8**) (furosemide – bipyrindyl – ethylene glycol) (1:1:0.5). (Key: as for Figure S2)

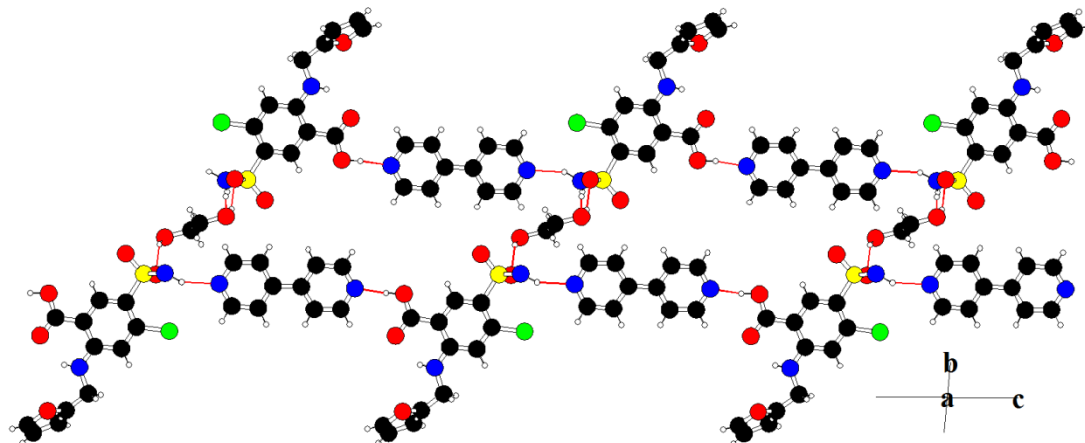


**Figure S10:** Packing arrangement in co-crystal (**8**) (furosemide – bipyrindyl – ethylene glycol) in [100] direction. (Key: as for Figure S3)



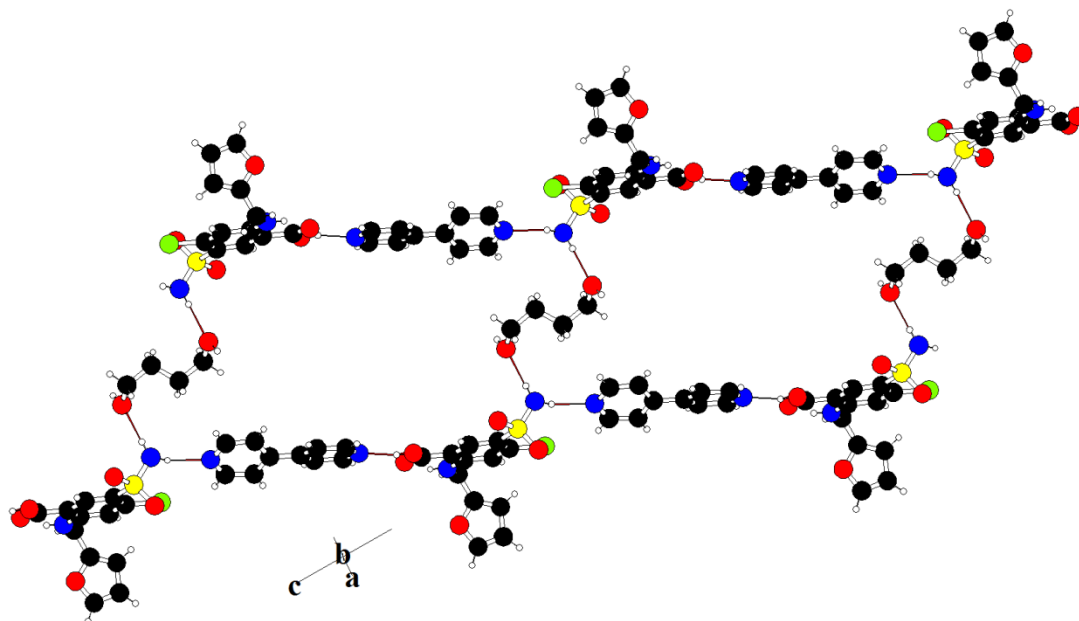


**Figure S13:** Packing arrangement in co-crystal (9) (furosemide – bipyriddy – 1,4-butanediol) in [010] direction. (Key: as for Figure S3)

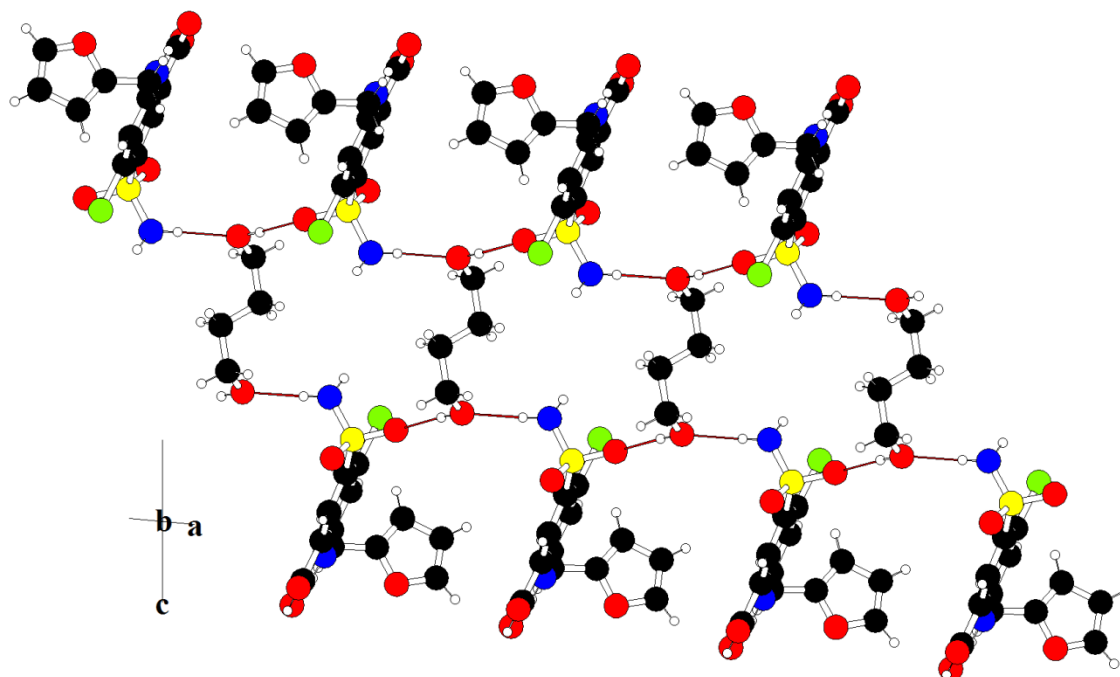


**Figure S14:** Packing arrangement in co-crystal (9) (furosemide – bipyriddy – 1,4-butanediol) in [010] direction. (Key: as for Figure S3)

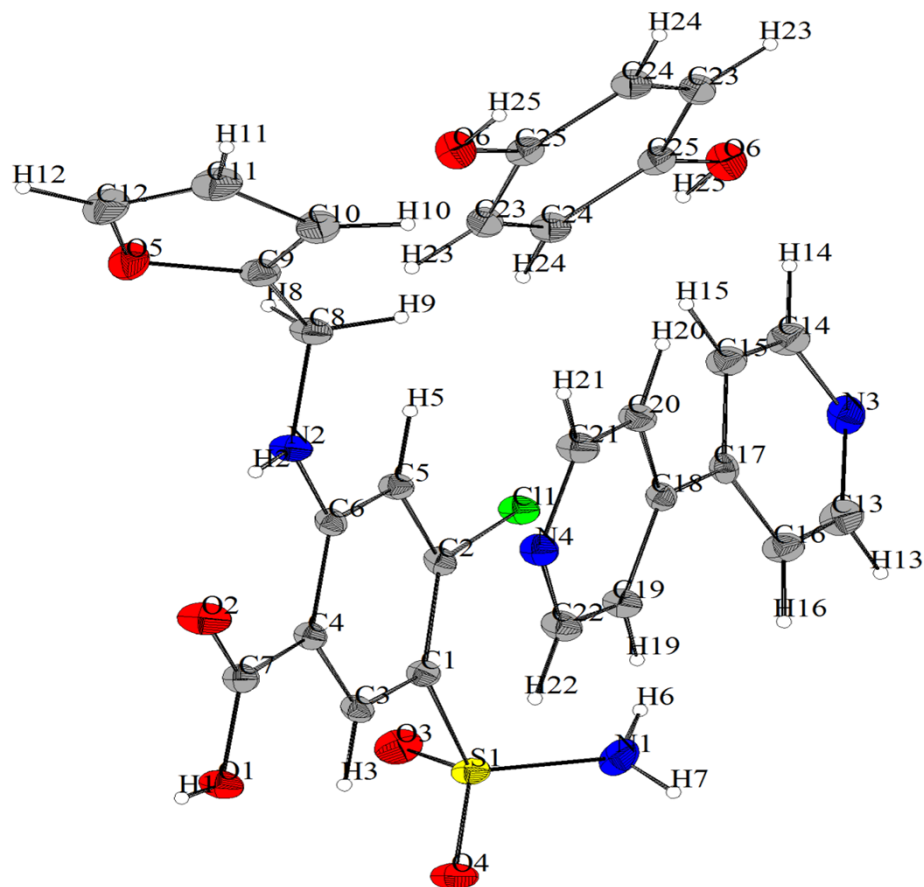


**Figure S15:** ORTEP picture of co-crystal (10) (furosemide – bipyridyl – hydroquinone) (1:1:0.5). (Key: as for Figure S2)

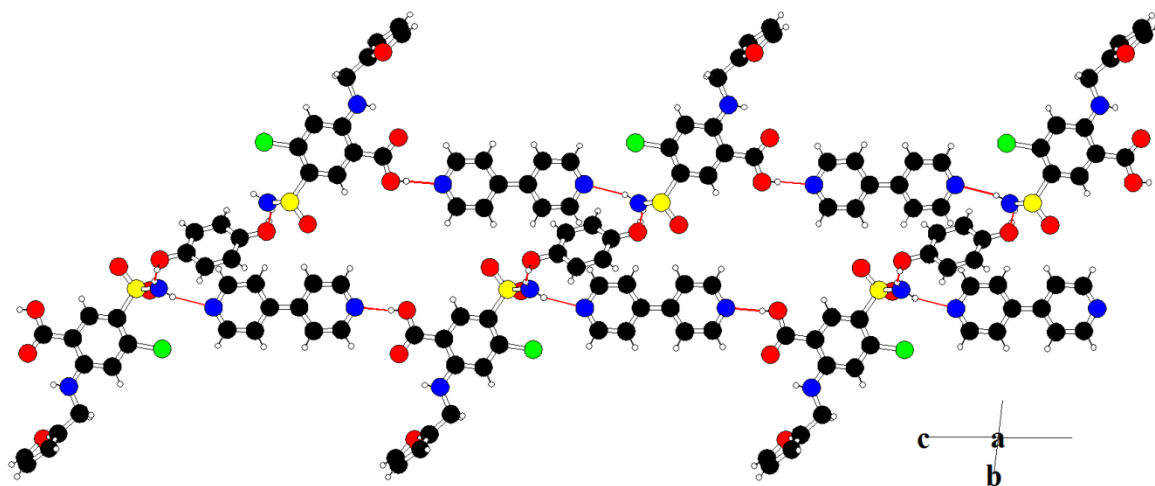


**Figure S16:** Packing arrangement in co-crystal (10) (furosemide – bipyridyl – 1,4-butanediol) in [100] direction. (Key: as for Figure S3)

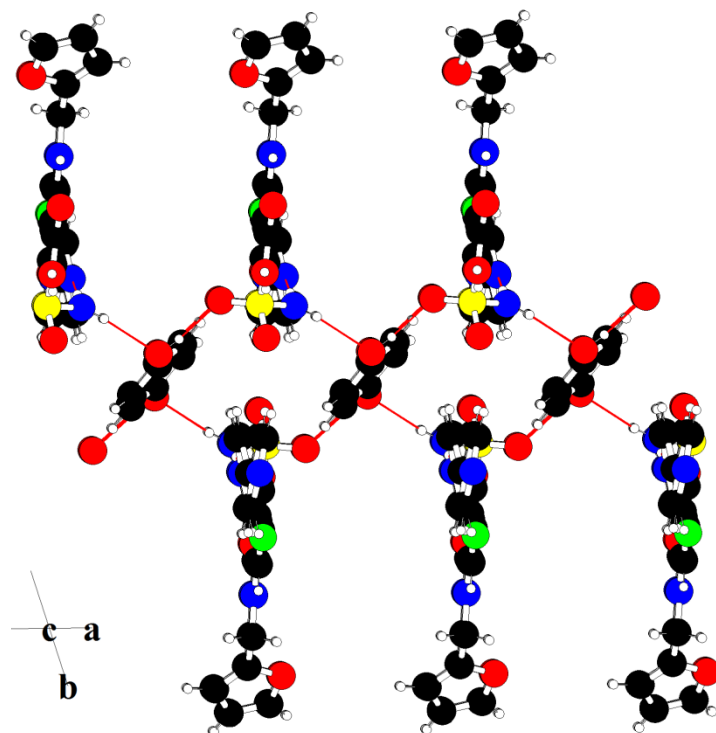


**Figure S17:** Packing arrangement in co-crystal (**10**) (furosemide – bipyriddyol – 1,4-butanediol) in [001] direction. (Key: as for Figure S3)

#### 4 Powder pattern fitting for co-crystals (4) - (7) and resulting unit cell parameters

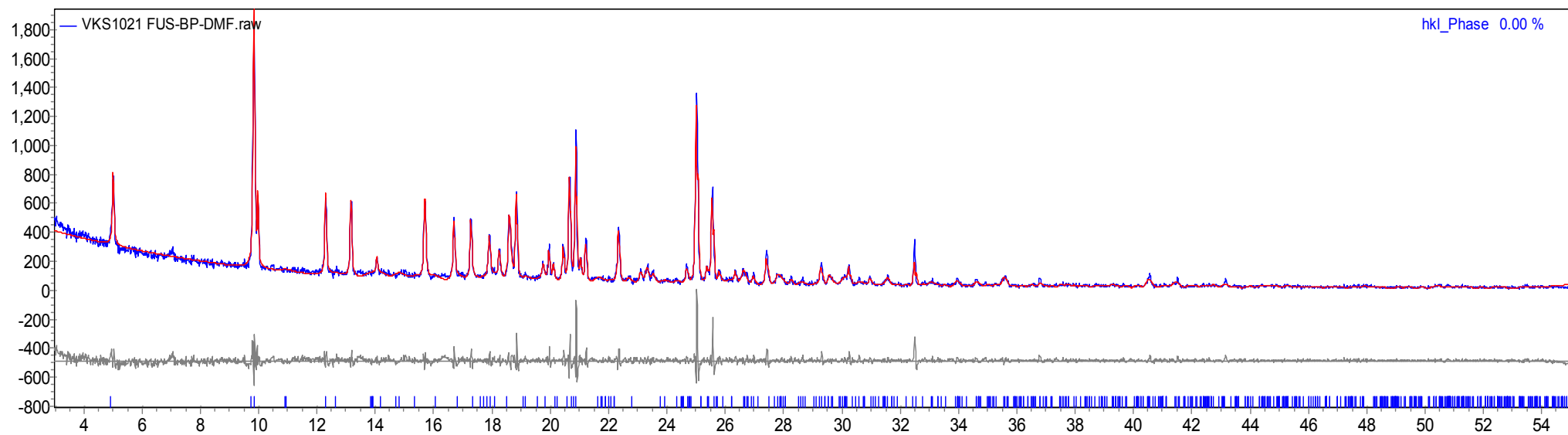


**Figure S18.** Powder pattern fitting for co-crystal (4) (furosemide – bipyridyl – DMF)

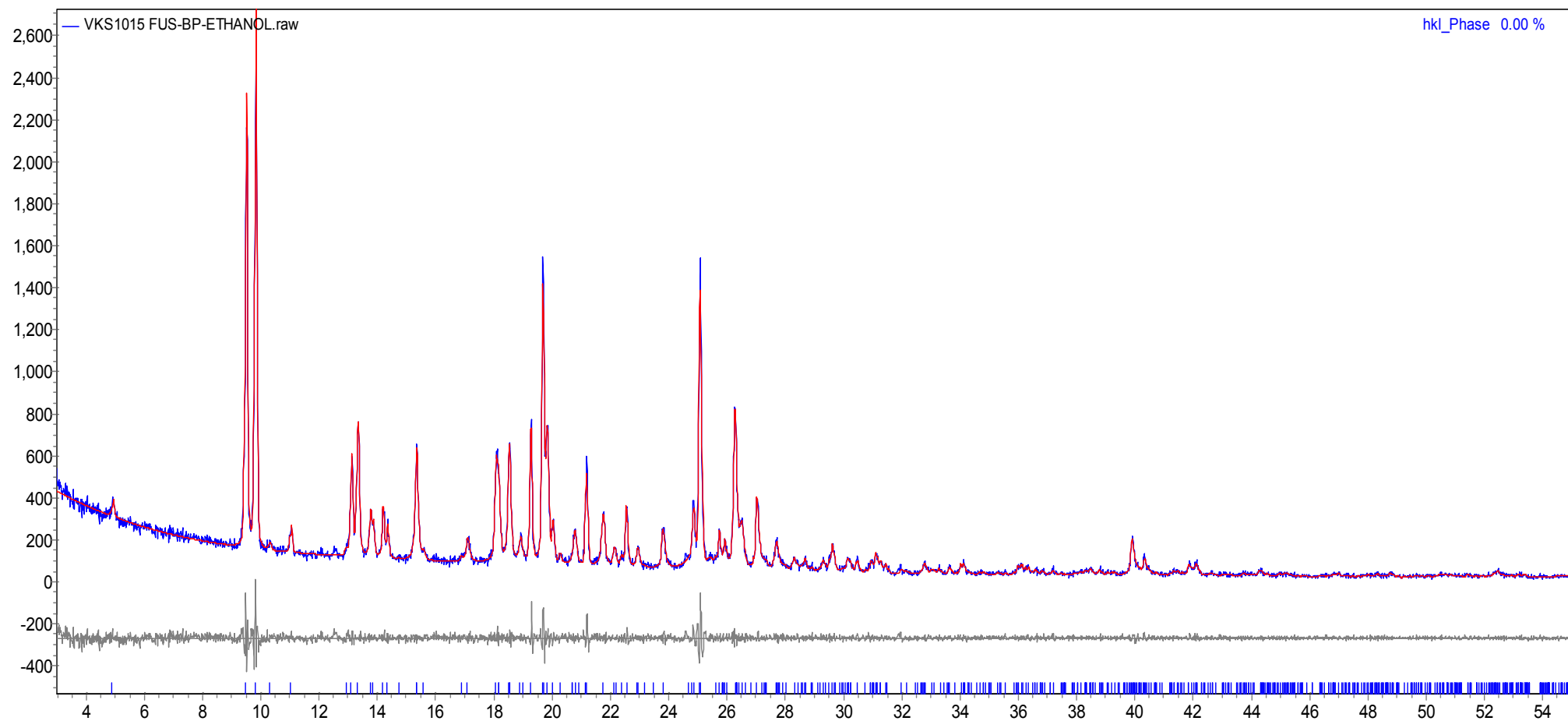


**Figure S19.** Powder pattern fitting of co-crystal (5) (furosemide – bipyridyl – ethanol)

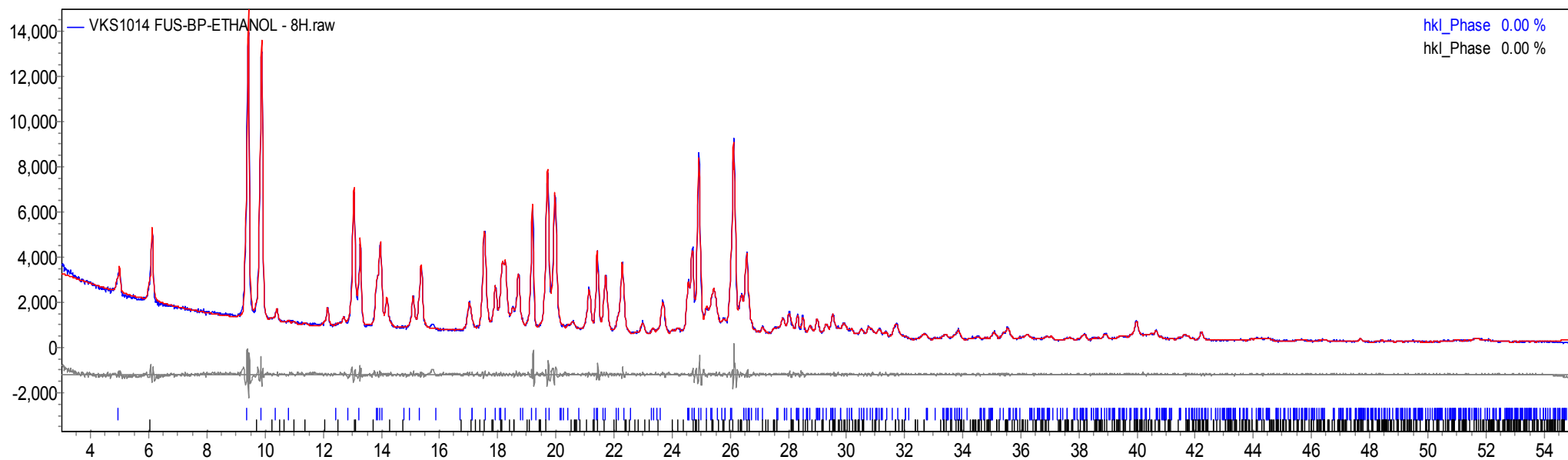


**Figure S20.** Powder pattern fitting of co-crystal (6) (furosemide – bipyridyl – 2-propanol). The reflections marked in blue correspond to the co-crystal (6), whilst the reflections marked in black correspond to unreacted furosemide (unit cell parameters:  $a=10.467(12)$ ,  $b=15.801(15)$ ,  $c=9.584(10)$  Å,  $\alpha=71.87$ ,  $\beta=115.04$ ,  $\gamma=108.48$  °)

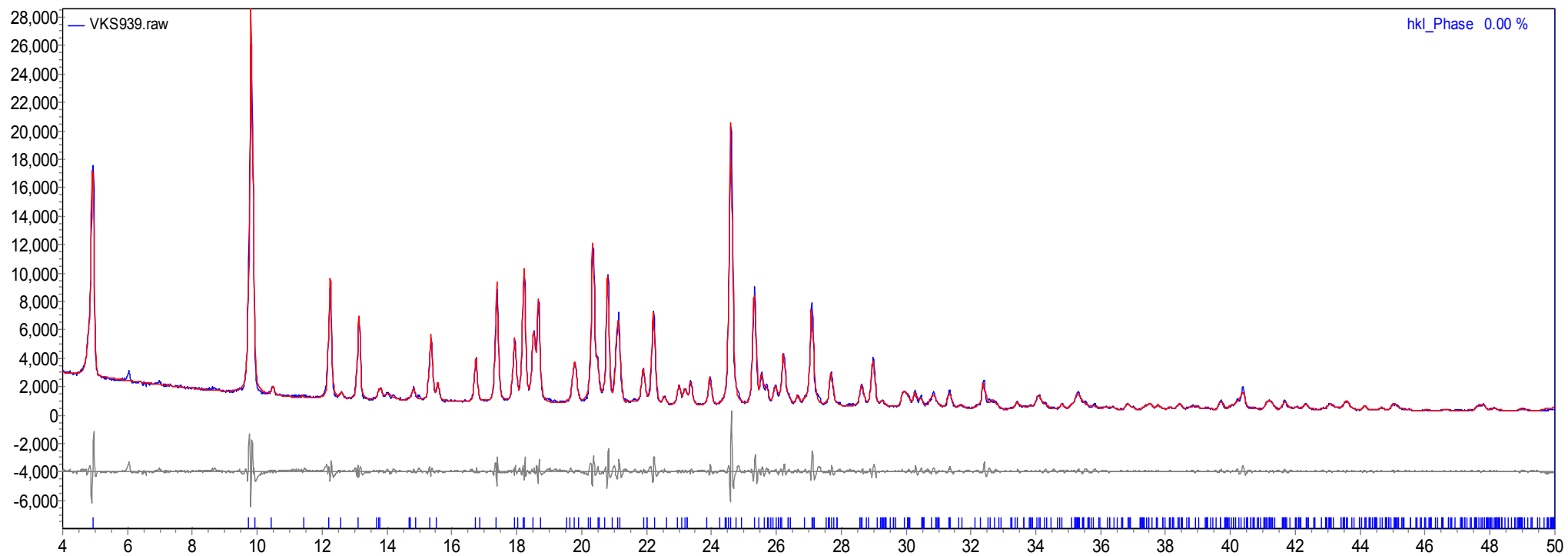


**Figure S21.** Powder pattern fitting of co-crystal (7) (furosemide – bipyridyl – 1-butanol)

**Table S1:** Unit cell parameters of co-crystals (4), (5) – (7) from powder diffraction patterns.

	(4)	(5)	(6)	(7)
Chemical formula	C <sub>25</sub> H <sub>26</sub> Cl <sub>1</sub> N <sub>5</sub> O <sub>5</sub> S	C <sub>24</sub> H <sub>25</sub> Cl <sub>1</sub> N <sub>4</sub> O <sub>6</sub> S	C <sub>25</sub> H <sub>27</sub> Cl <sub>1</sub> N <sub>4</sub> O <sub>6</sub> S	C <sub>26</sub> H <sub>29</sub> Cl <sub>1</sub> N <sub>4</sub> O <sub>6</sub> S
Formula weight	544.2	533.0	547.0	561.0
Crystal system	triclinic	triclinic	triclinic	triclinic
<i>a</i> / Å	7.452(2)	7.193(8)	7.860(5)	7.537(4)
<i>b</i> / Å	9.315(5)	9.780(6)	10.001(2)	9.374(3)
<i>c</i> / Å	18.557(7)	18.694(2)	18.402(4)	18.282(2)
$\alpha$ / °	87.16(9)	89.88(5)	76.13(1)	81.67(7)
$\beta$ / °	74.80(1)	75.50(3)	76.56(5)	80.54(5)
$\gamma$ / °	76.94(4)	73.17(1)	70.94(2)	75.6(3)
Space group	<i>P</i> $\bar{1}$	<i>P</i> $\bar{1}$	<i>P</i> $\bar{1}$	<i>P</i> $\bar{1}$
<i>V</i> / Å <sup>3</sup>	1213.95(3)	1208.96(5)	1257.41(2)	1226.57(8)
FOM	25.9	7.8	5.5	7.2
R <sub>wp</sub> / %	7.29	8.64	5.62	4.95



T / K	100	100	100	100	100	100
$\theta$ range/ $^{\circ}$	3 – 44	4 – 34	1 – 40	1 – 34	1 – 37	1 – 29
Range of $h$	-22 – 22	-15 – 15	-12 – 12	-10 – 10	-12 – 12	-9 – 9
Range of $k$	-16 – 18	-16 – 16	-14 – 15	-14 – 14	-15 – 12	-13 – 12
Range of $l$	-31 – 31	-21 – 21	-31 – 31	0 – 29	-30 – 30	-24 – 25
Rmerge	0.0455	0.0263	0.0305	0.0360	0.0399	0.0239
$R_1$ / %	4.26516	4.46	4.17	6.73	3.76	4.36
$wR_2$ / %	4.64728	4.5	4.47	6.40	4.22	3.66
Goodness-of-fit	1.076	1.118	1.077	0.965	1.030	1.098

**Table S3:** Geometric aspects of co-crystals **(1)**, **(2)**, **(3)**, **(8)** – **(10)**:

Compound	Hydrogen bond	$d(\text{H}\cdots\text{A})/\text{\AA}$	$d(\text{D}\cdots\text{A})/\text{\AA}$	$\theta(\text{D-H}\cdots\text{A})/^\circ$	(H $\cdots$ A) van der Waals' cutoff contraction / %
<b>1</b>	O(1)-H(1) $\cdots$ N(3)	1.57	2.53	166.5	43
	N(2)-H(2) $\cdots$ O(1)	2.15	2.97	157.2	21
	N(2)-H(3) $\cdots$ O(2)	2.04	1.93	169.2	25
<b>1(intra)</b>	N(1)-H(6) $\cdots$ O(2)	2.00	2.67	134.6	26
<b>2</b>	N(1)-H(6) $\cdots$ N(3)	2.11	2.99	160.9	23
	N(1)-H(7) $\cdots$ O(6)	2.13	2.91	172.0	22
	O(1)-H(1) $\cdots$ N(4)	1.75	2.56	174.7	36
	C(24)-H(28) $\cdots$ O(4)	2.53	3.38	147.0	7
<b>2</b>	C(23)-H(25) $\cdots$ O(3)	2.51	3.40	166.4	8
<b>2(intra)</b>	N(2)-H(2) $\cdots$ O(2)	2.00	2.69	139.5	26
<b>3</b>	N(1)-H(6) $\cdots$ N(3)	2.18	2.97	162.4	21
	N(1)-H(7) $\cdots$ O(6)	2.02	2.89	169.1	26
	O(6)-H(25) $\cdots$ O(3)	1.97	2.77	161.4	27
	O(1)-H(1) $\cdots$ N(4)	1.84	2.62	173.2	33
<b>3(intra)</b>	N(2)-H(2) $\cdots$ O(2)	1.99	2.66	138.5	27
<b>8</b>	O(1)-H(1) $\cdots$ N(4)	1.69	2.60	150.9	38
	N(1)-H(6) $\cdots$ N(3)	1.98	2.91	152.7	28
	N(1)-H(7) $\cdots$ O(6)	2.09	2.93	166.2	23
	O(6)-H(25) $\cdots$ O(3)	2.02	2.78	153.5	26
<b>8(intra)</b>	N(2)-H(2) $\cdots$ O(2)	2.00	2.66	139.8	26
<b>9</b>	O(1)-H(1) $\cdots$ N(3)	1.81	2.62	169.5	34
	N(1)-H(6) $\cdots$ N(4)	2.11	2.97	160.2	23
	O(6)-H(25) $\cdots$ O(4)	1.89	2.75	176.0	30
	N(1)-H(7) $\cdots$ O(6)	2.01	2.88	171.7	26
<b>9(intra)</b>	N(2)-H(2) $\cdots$ O(2)	1.97	2.66	137.1	27
<b>10</b>	O(1)-H(1) $\cdots$ N(4)	1.83	2.61	173.6	33
	N(1)-H(6) $\cdots$ N(3)	2.12	2.92	162.4	23
	N(1)-H(7) $\cdots$ O(6)	2.14	2.95	157.9	21
	O(6)-H(25) $\cdots$ O(3)	1.87	2.70	173.6	31
<b>10(intra)</b>	N(2)-H(2) $\cdots$ O(2)	2.02	2.65	138.1	26

## 6 Thermal analysis data for co-crystals (1) – (3), (8) – (10).

All the DSC and DTA traces are reported with endothermic and exothermic transitions directed towards and away from the x-axis respectively

The DSC thermogram of co-crystal (1) (Figure S23) shows an endothermic transition with an onset temp of 222.9°C, corresponding to the melting of co-crystal (1). The melting transition temp of co-crystal (1) is different from the melting transition temperatures of furosemide (melting point – 218 to 220°C) and 4,4'-bipyridyl (melting point (119 to 121°C))

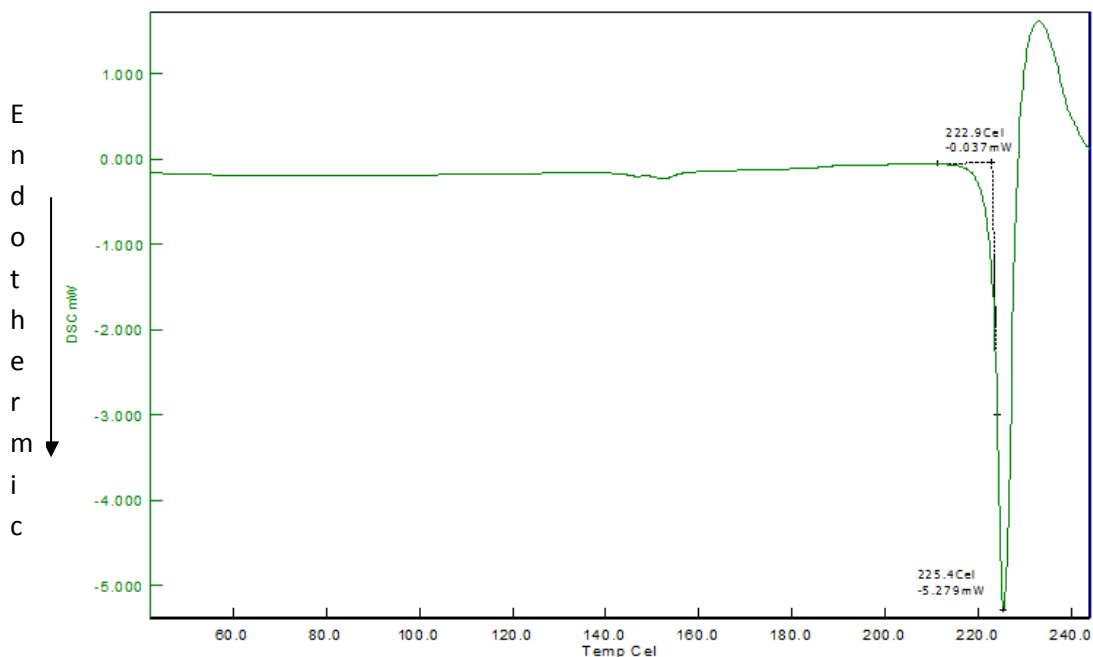


**Figure S23** DSC of co-crystal (1) (furosemide-bipyridyl (1:0.5))

The TG/DTA of co-crystal (**2**) is shown in Figure S24. The TG thermogram shows a weight loss of 15.2%, corresponding to the loss of one mole of DMSO. This weight loss in the TG curve is seen as an endothermic transition in the DTA curve with an onset of 117.2°C. The loss of DMSO molecule is immediately followed by a loss of 10.9%, which may be assigned to the loss of half a molecule of 4,4'-bipyridyl. This transition is followed by a transition corresponding to the melting of the material with an onset temp of 217.7°C. The transitions following may be due to the decomposition of the material, observed as abrupt weight loss in the TG curve.

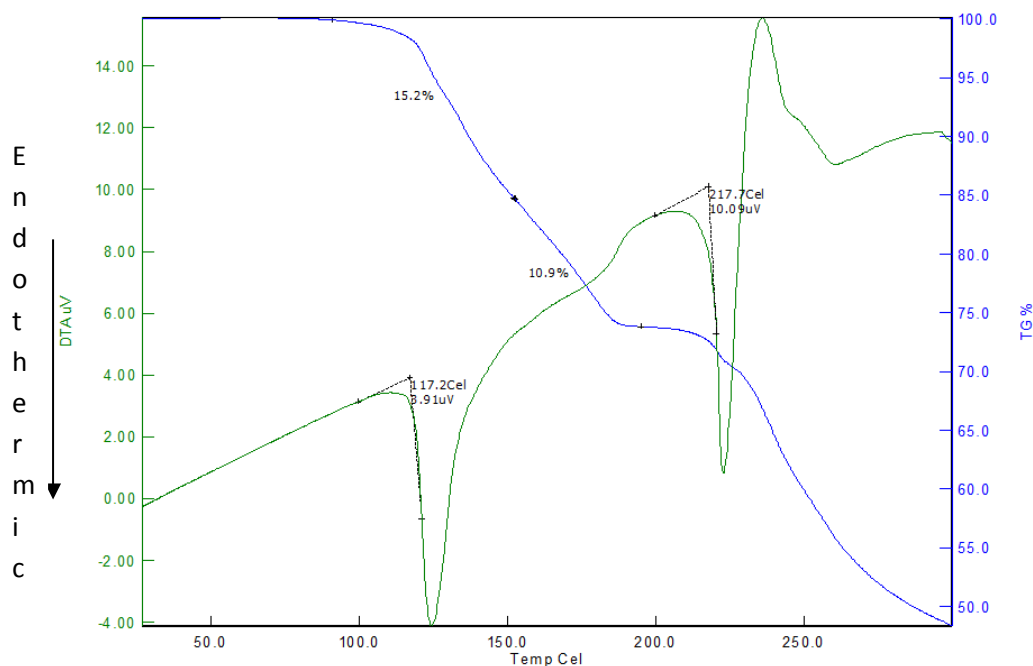


**Figure S24** TGA/DTA of co-crystal (**2**) (furosemide – bipyridyl – DMSO)

The TG/DTA of co-crystal (**3**) is shown in Figure S25. The TG thermogram indicates an initial weight loss of 7.2% between *ca.*50- 150°C, corresponding to the loss of one mole of methanol from the crystal lattice. The weight loss in the TG curve is seen as an endothermic transition in the DTA curve with an onset temp of 90.9°C. This is followed by a transition corresponding to the melting of the compound, with an onset of 219.5°C. The transitions following are due to the decomposition of the material.

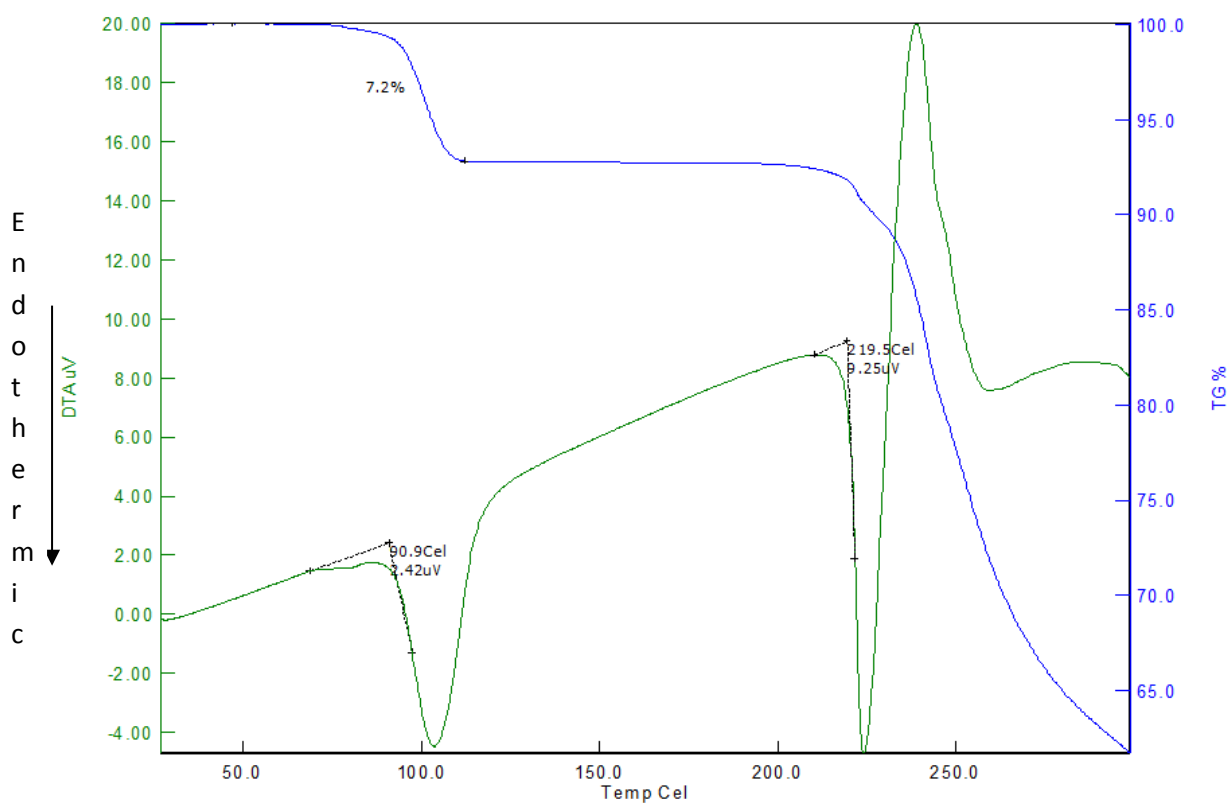


**Figure S25** TGA/DTA of co-crystal (**3**) (furosemide – bipyridyl – MeOH)

The TG/DTA data of co-crystal (**8**) is shown in Figure S26. The TG data shows an initial weight loss of 4.9% corresponding to the loss of surface bound ethylene glycol molecules. This is followed by a weight loss of 6.9%, corresponding to the loss of half molecule of ethylene glycol from the crystal lattice. The loss of half molecule of ethylene glycol in the TG curve is seen as a sharp endothermic transition in the DTA thermogram with an onset temp of 110.0°C. This is followed in the DTA curve by a transition corresponding to melting of the compound with an onset temp of 216.8°C, seen as an endothermic transition. The melting transition is immediately followed by transitions corresponding to the decomposition of the compound.

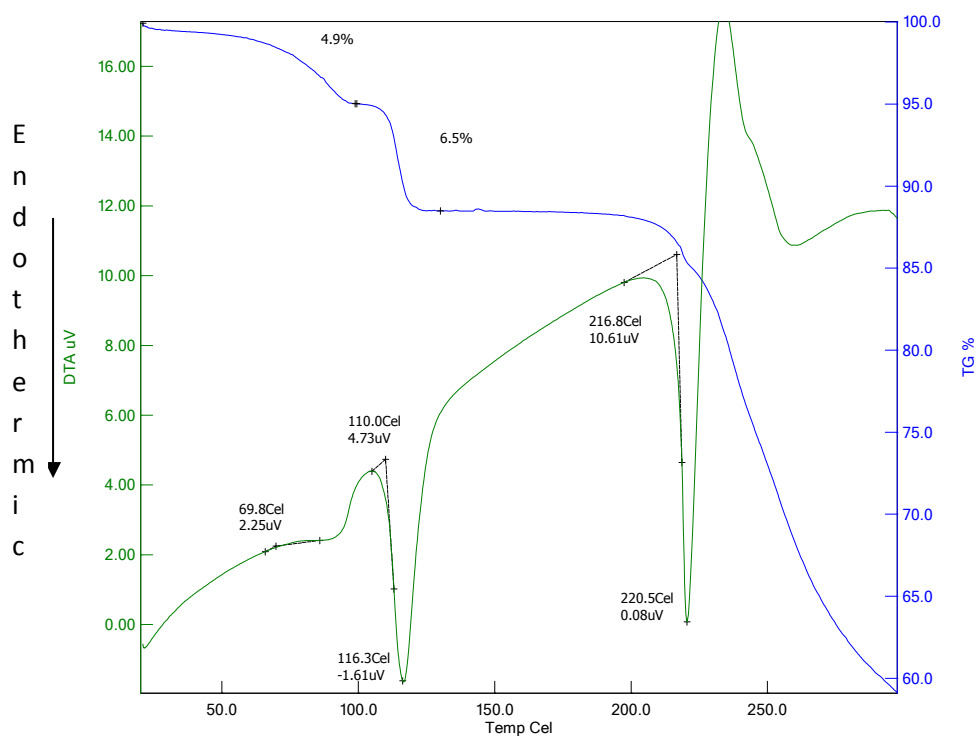


**Figure S26** TGA/DTA of co-crystal (**8**) (furosemide – bipyridyl – ethylene glycol).

The TG/DTA data of co-crystal (9) is shown in Figure S27. The TG thermogram of co-crystal (9) shows a weight loss of 8.9%, which could be due to the loss of half molecule of 1,4-butanediol from the crystal lattice. This is observed as a broad endothermic transition in the DTA curve with onset temp of 100.1°C. This loss of half molecule of 1,4-butanediol is followed by a weight loss of 21.8°C, which is consistent with the loss of half a molecule of 4,4'-bipyridyl, seen as a sharp endothermic transition in the DTA curve with an onset temp of 159.4°C. This is followed by a transition corresponding to the melting of the compound, with an onset temp of 207.2°C.

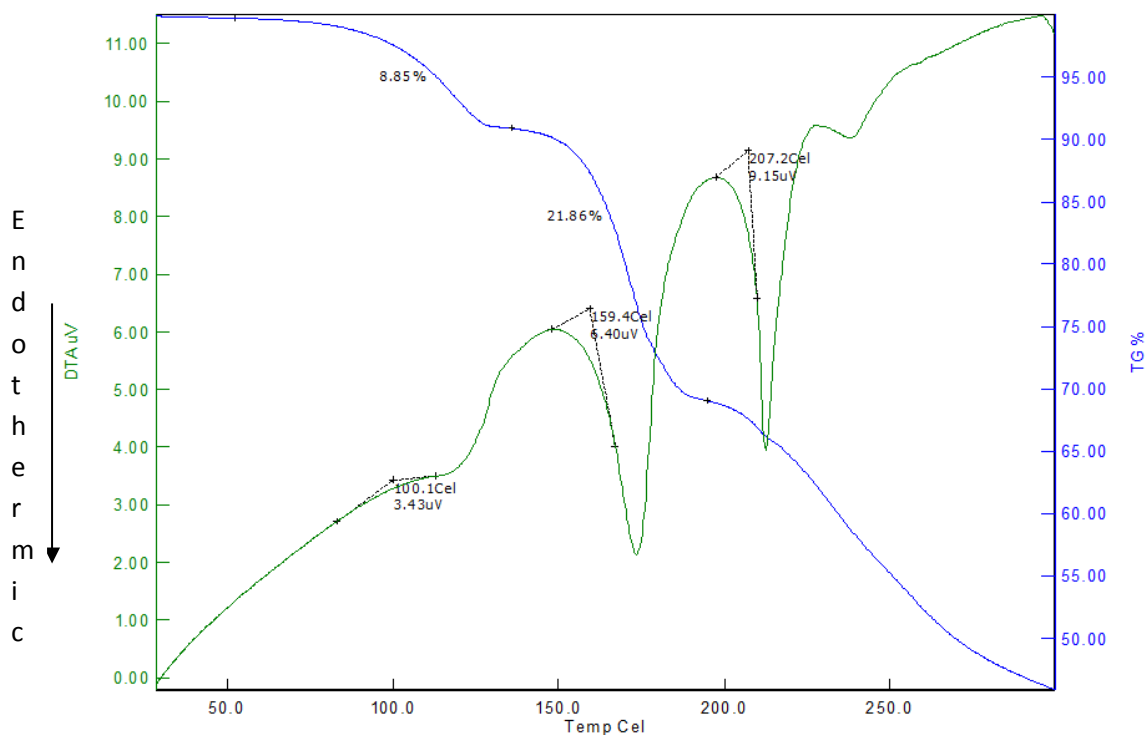


**Figure S27** TGA/DTA of co-crystal (9) furoseamide – bipyridyl – 1,4-butanediol.

The DSC of co-crystal (**10**) is shown in Figure S28. The DSC of the material shows a sharp endothermic transition with an onset temp of 207.4oC, which is different from any of the starting materials (furosemide (mp – 219 to 220oC) ; 4,4'-bipyridyl (mp – 119 to 121°C); hydroquinone (mp – 171 -173°C)).

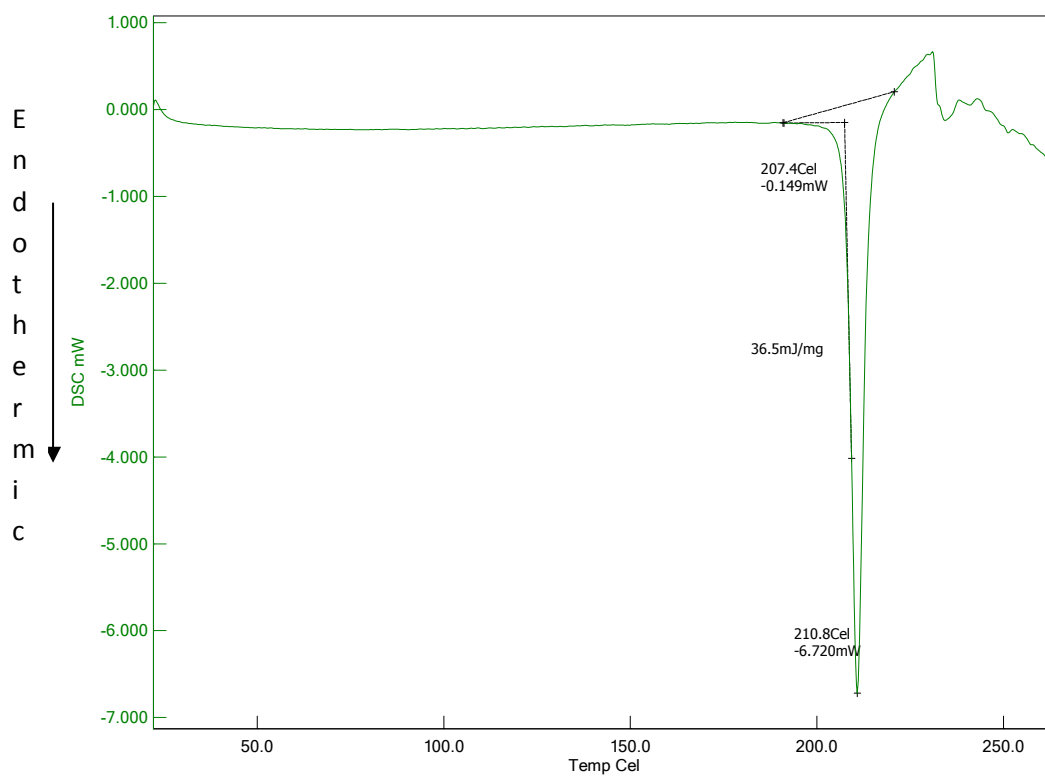


**Figure S28** DSC of co-crystal (**10**) (furosemide – bipyridyl – hydroquinone).

**7 Spectroscopic data for co-crystals (1) – (3), (8) – (10).**

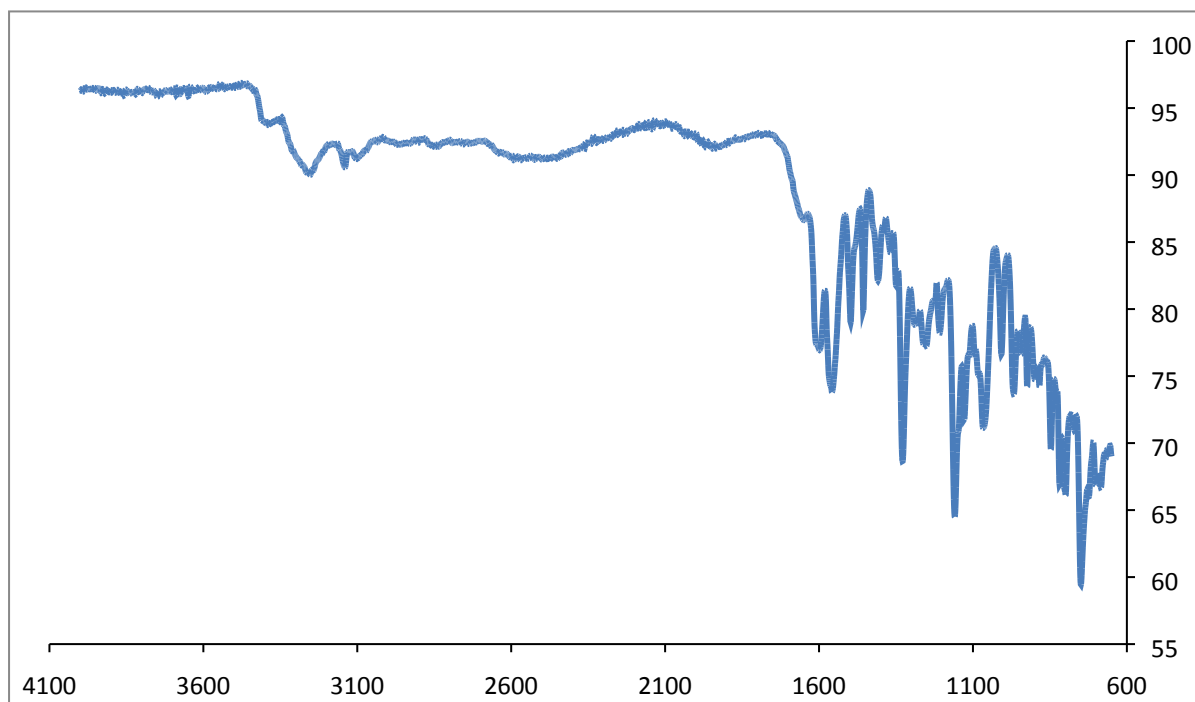


**Figure S29** Infrared spectrum of co-crystal (1) furosemide – bipyridyl (1:0.5).

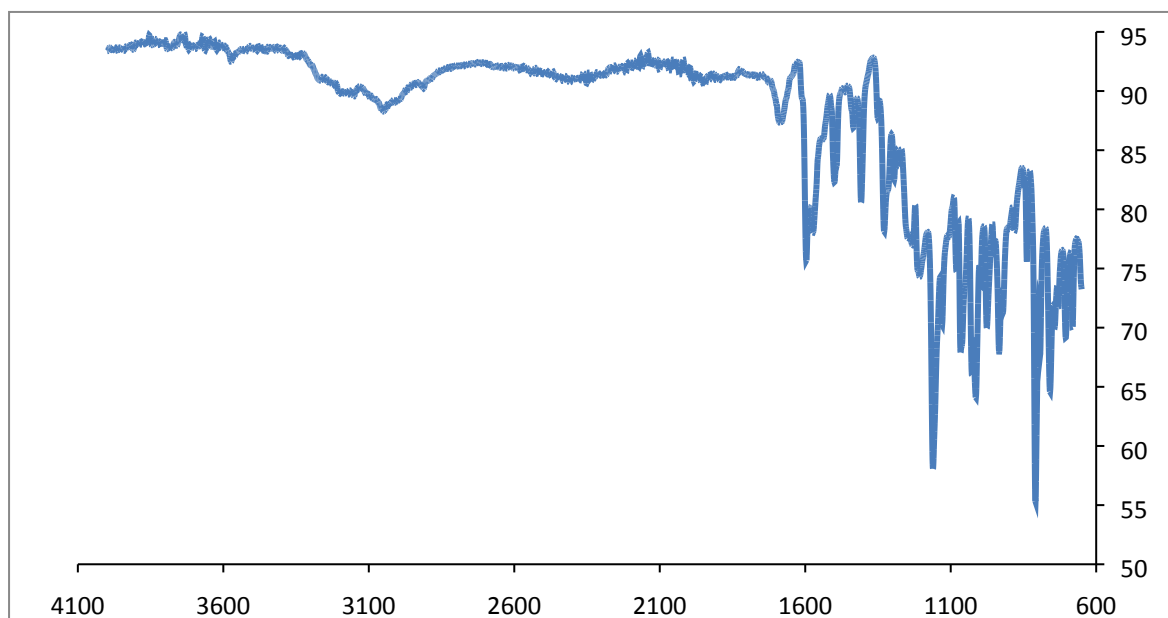


**Figure S30** Infrared spectrum of co-crystal (2) furosemide – bipyridyl – DMSO.

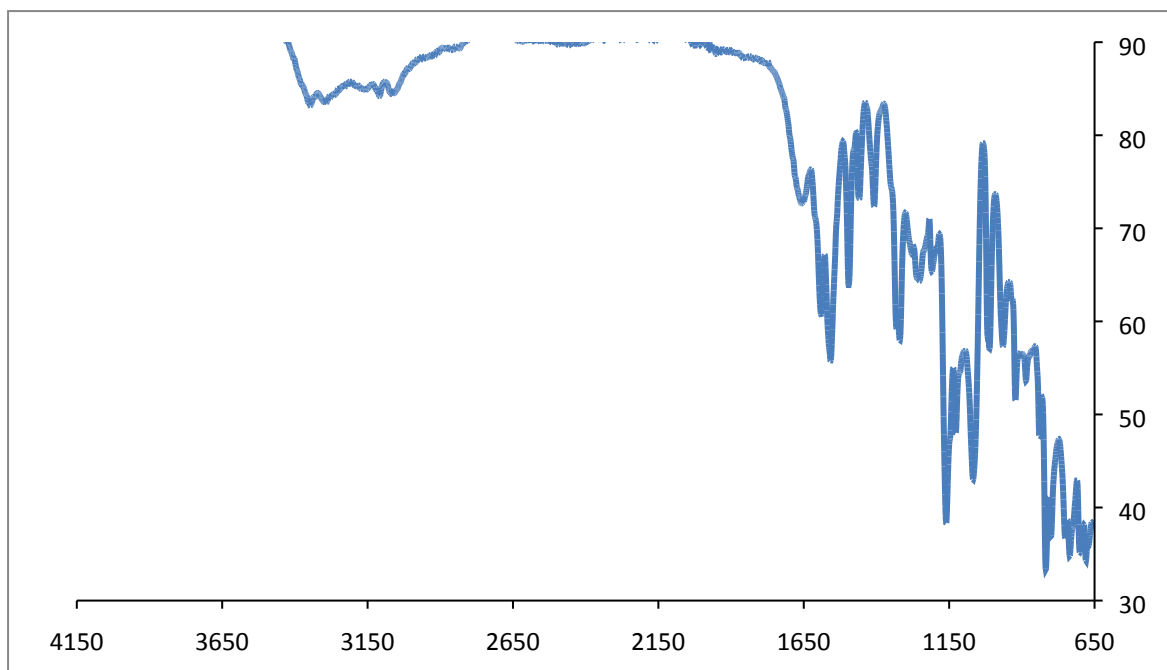


**Figure S31** Infrared spectrum of furosemide – bipyridyl – MeOH (**3**).

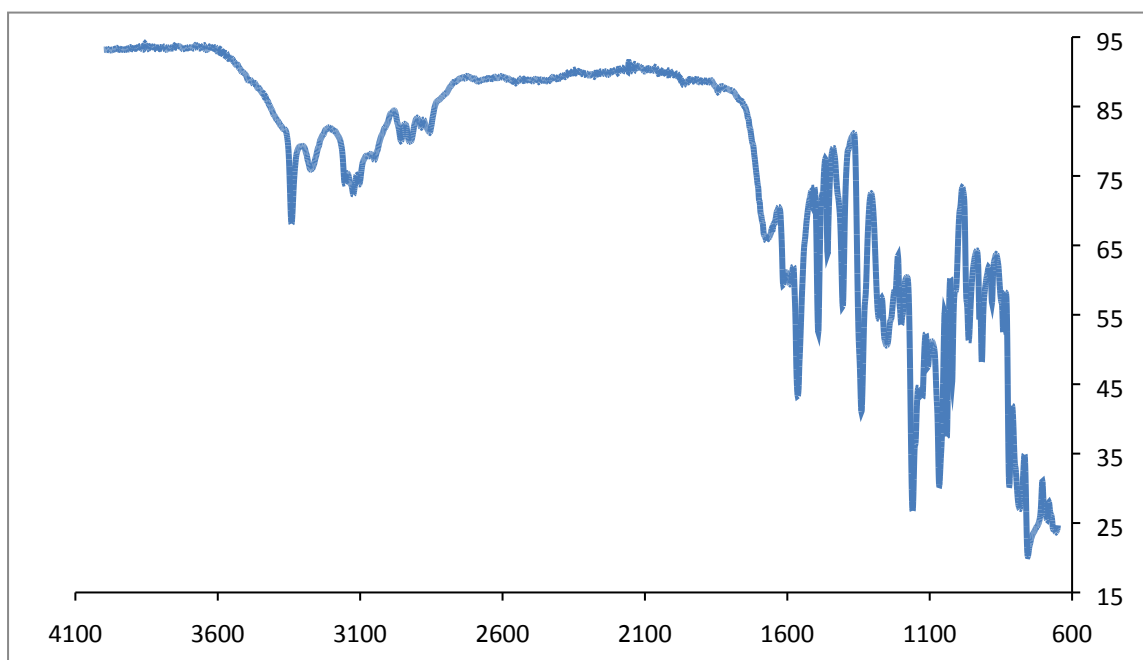


**Figure S32** Infrared spectrum of furosemide – bipyridyl – ethylene glycol (**8**).

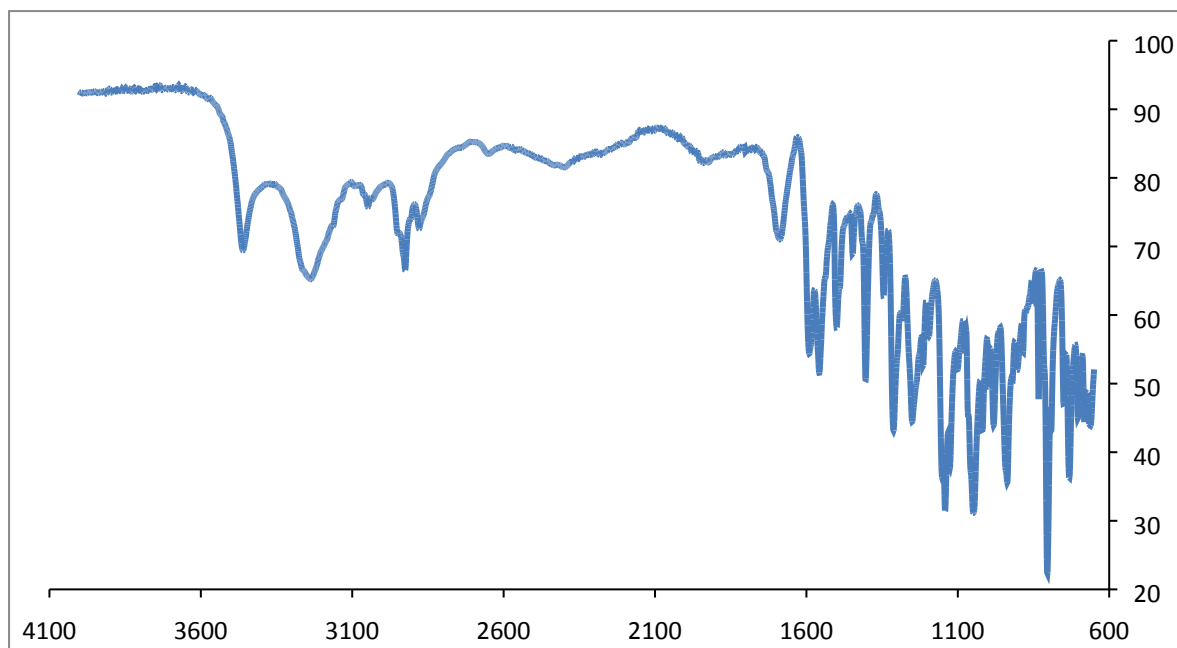


**Figure S33** Infrared spectrum of furosemide – bipyridyl – 1,4-butanediol (**9**).

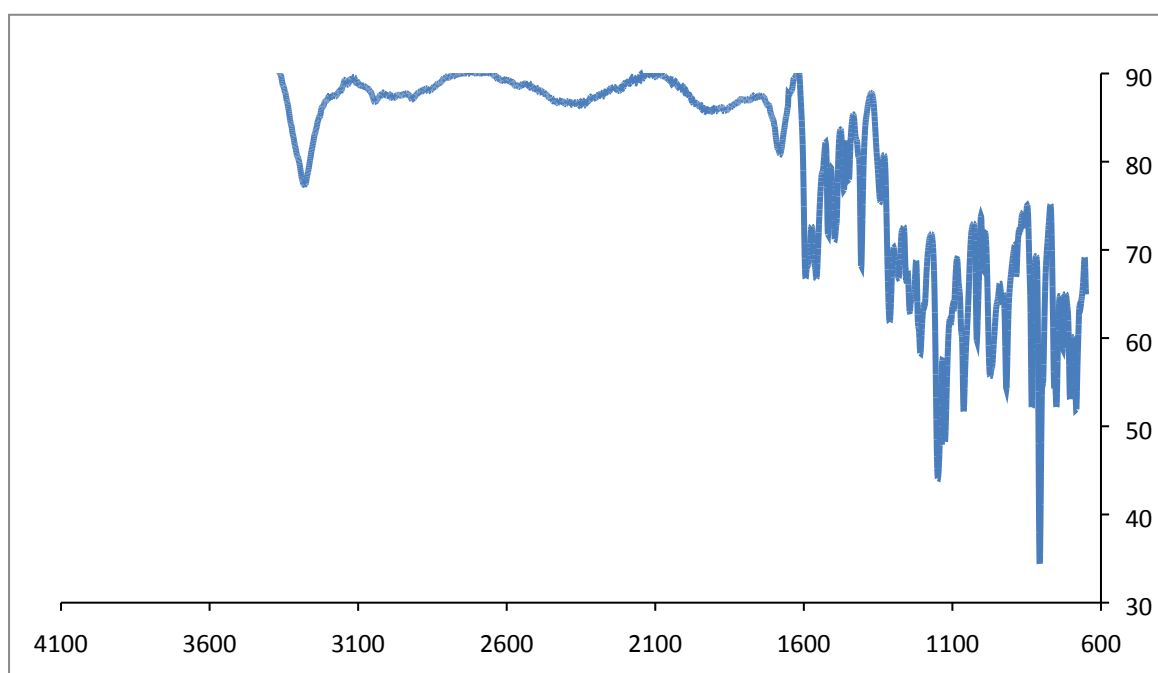
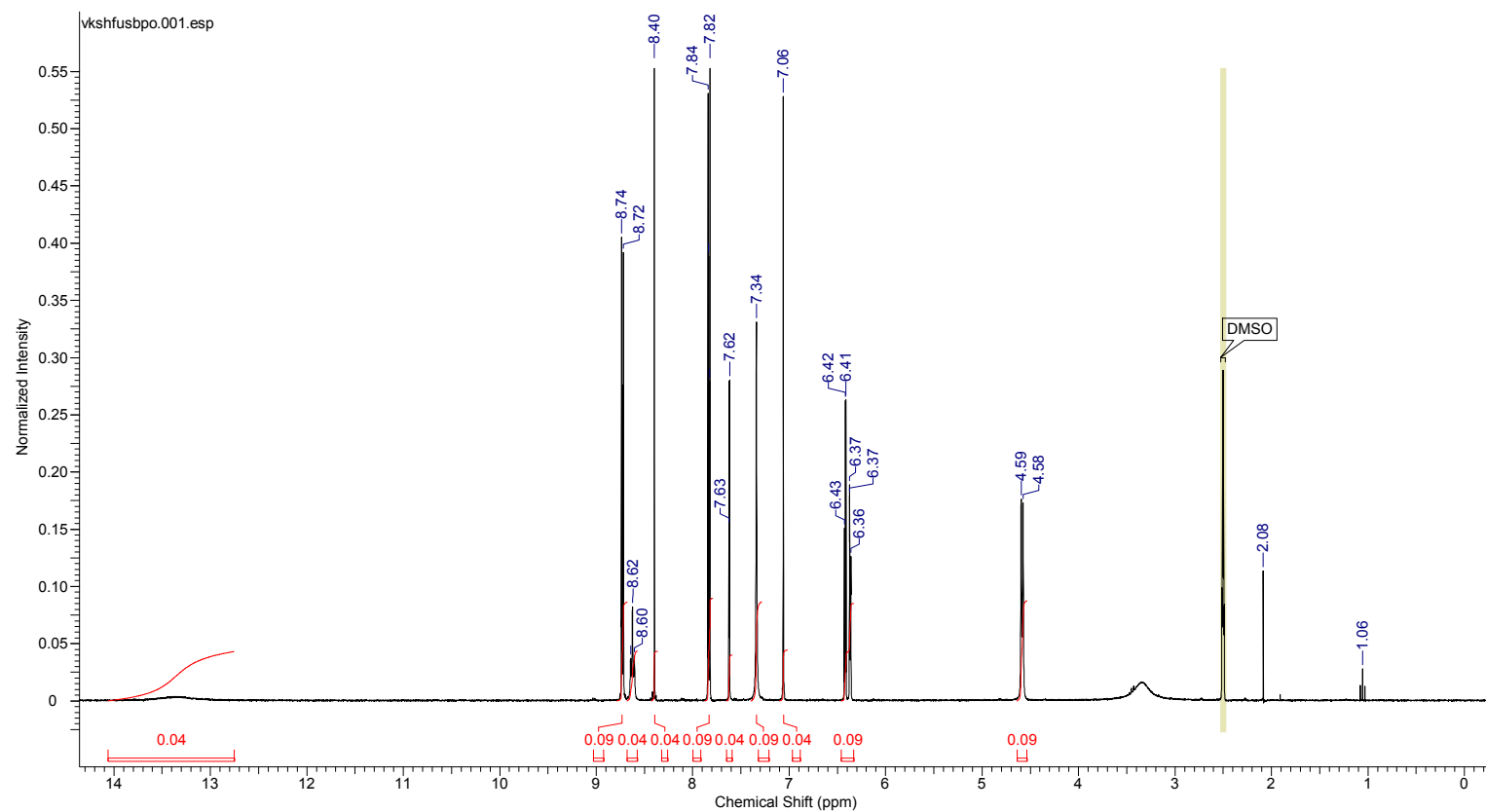


**Figure S34** Infrared spectrum of furosemide – bipyridyl – hydroquinone (**10**).

$^1\text{H-NMR}$  spectra:

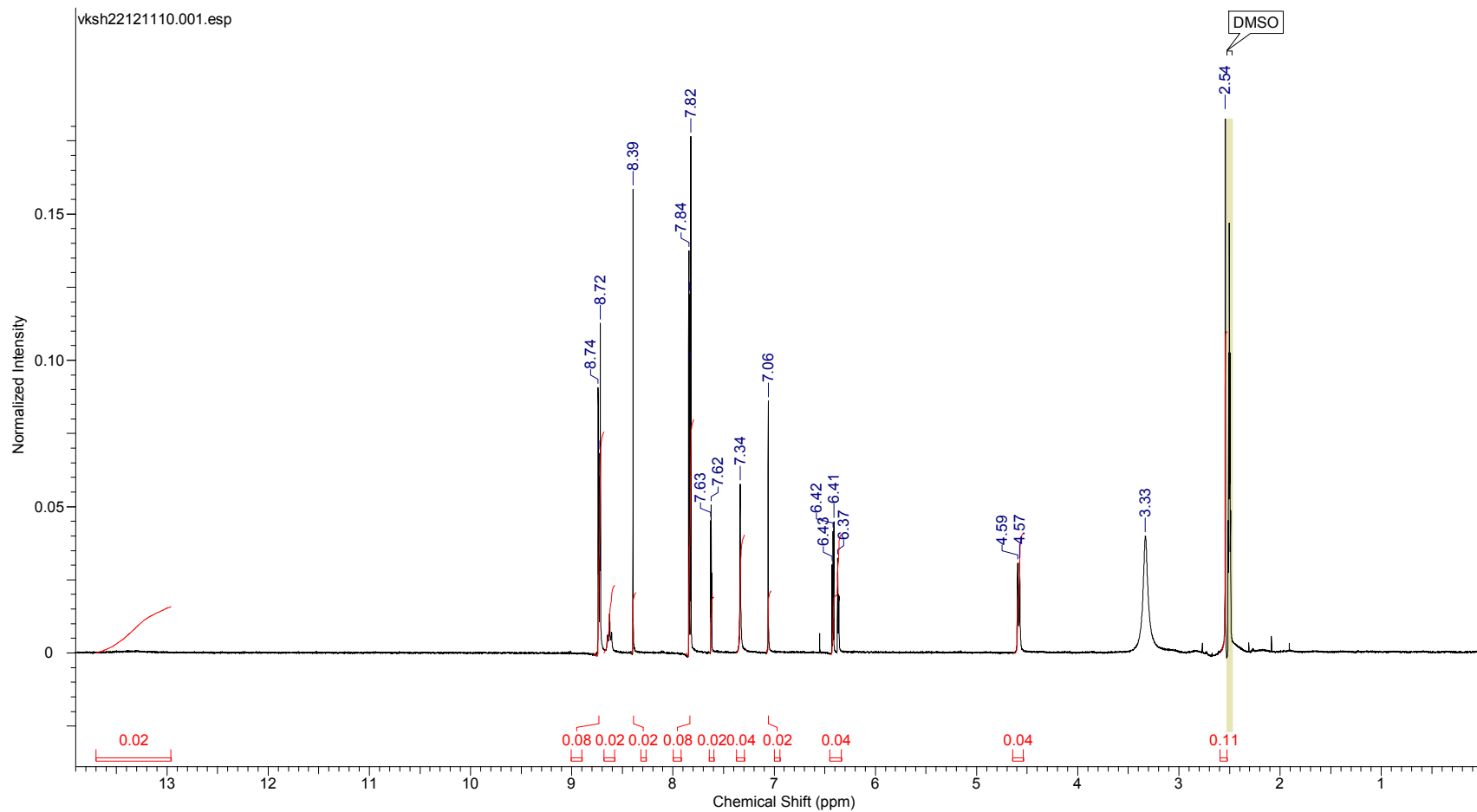
$^1\text{H-NMR}$  (300 MHz,  $\text{DMSO-d}_6$ ) of co-crystal (**1**) (furosemide-bipyridyl) (1:0.5)

The  $^1\text{H-NMR}$  of co-crystal (**1**) recorded in  $\text{DMSO-d}_6$  is shown below. The  $^1\text{H-NMR}$  confirms that the bulk material of co-crystal (**1**) is a representative of the single crystal analysed. The integral values suggests that the co-crystal (**1**) contains furosemide and 4,4'-bipyridyl in 1- 0.5 composition.



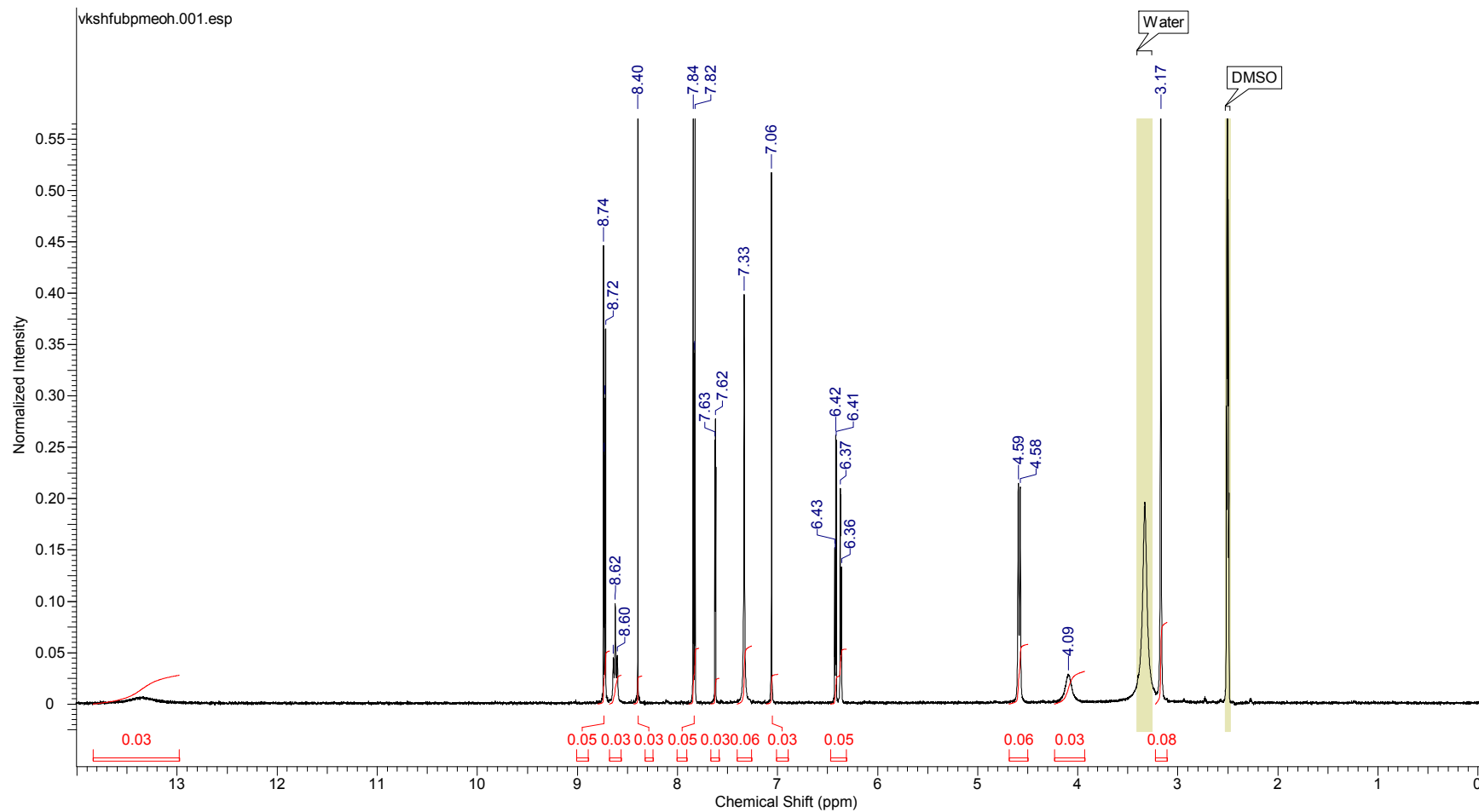
<sup>1</sup>H-NMR (300 MHz, DMSO-d<sub>6</sub>) of co-crystal (**2**) (furosemide-bipyridyl-DMSO)

The <sup>1</sup>H-NMR of co-crystal (**2**) recorded in DMSO-d<sub>6</sub> is shown below. The <sup>1</sup>H-NMR confirms that the bulk material of co-crystal (**2**) is a representative of the single crystal analysed. The integral values suggests that the co-crystal (**2**) contains furosemide, 4,4'-bipyridyl and the third component DMSO in 1-1-1 composition.



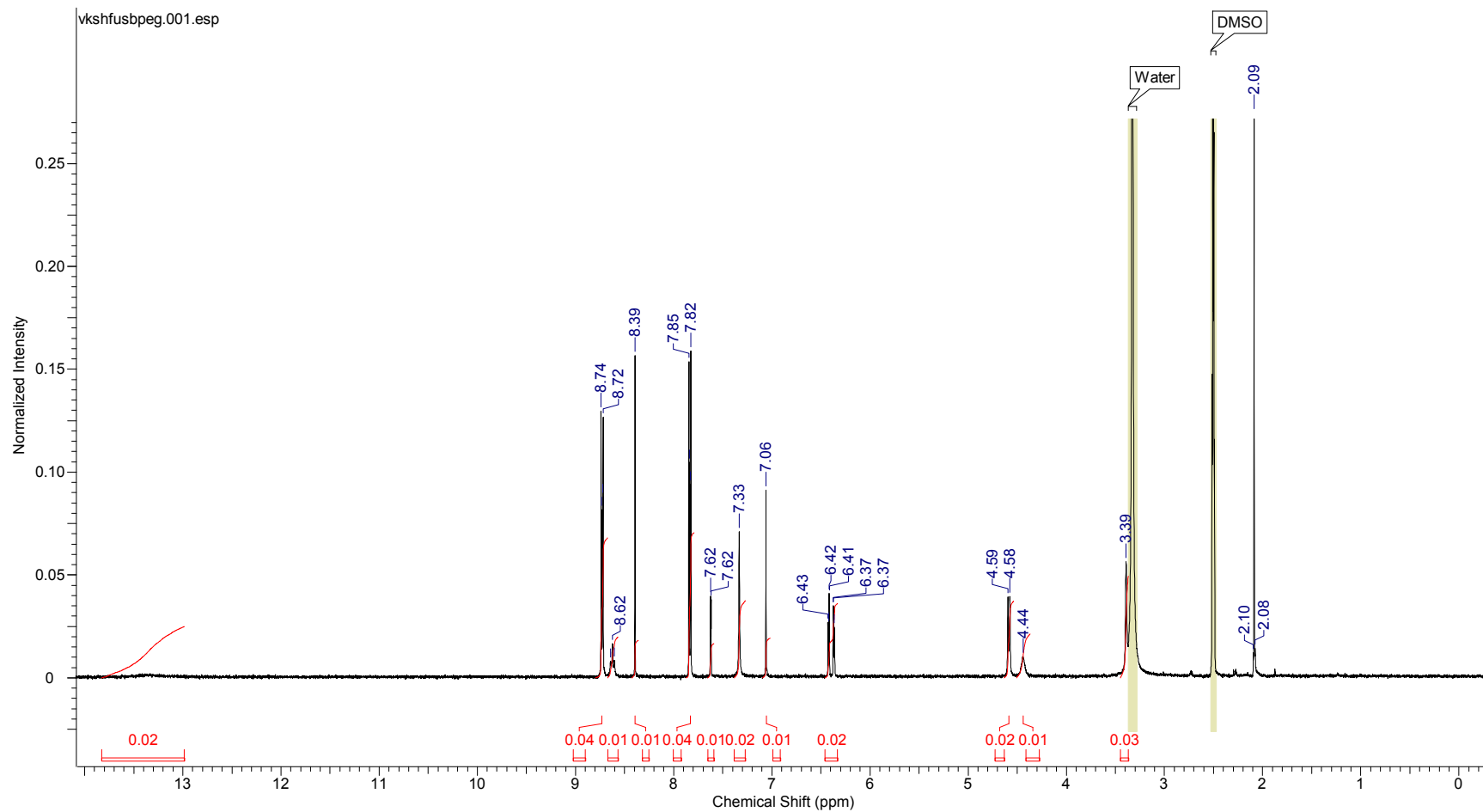
<sup>1</sup>H NMR (300 MHz, DMSO-d<sub>6</sub>) of co-crystals (**3**) (furosemide-bipyridyl-MeOH)

The <sup>1</sup>H-NMR of co-crystal (**3**) recorded in DMSO-d<sub>6</sub> is shown below. The <sup>1</sup>H-NMR confirms that the bulk material of co-crystal (**3**) is a representative of the single crystal analysed. The integral values suggests that the co-crystal (**3**) contains furosemide, 4,4'-bipyridyl and the third component methanol are in 1-1-1 composition.



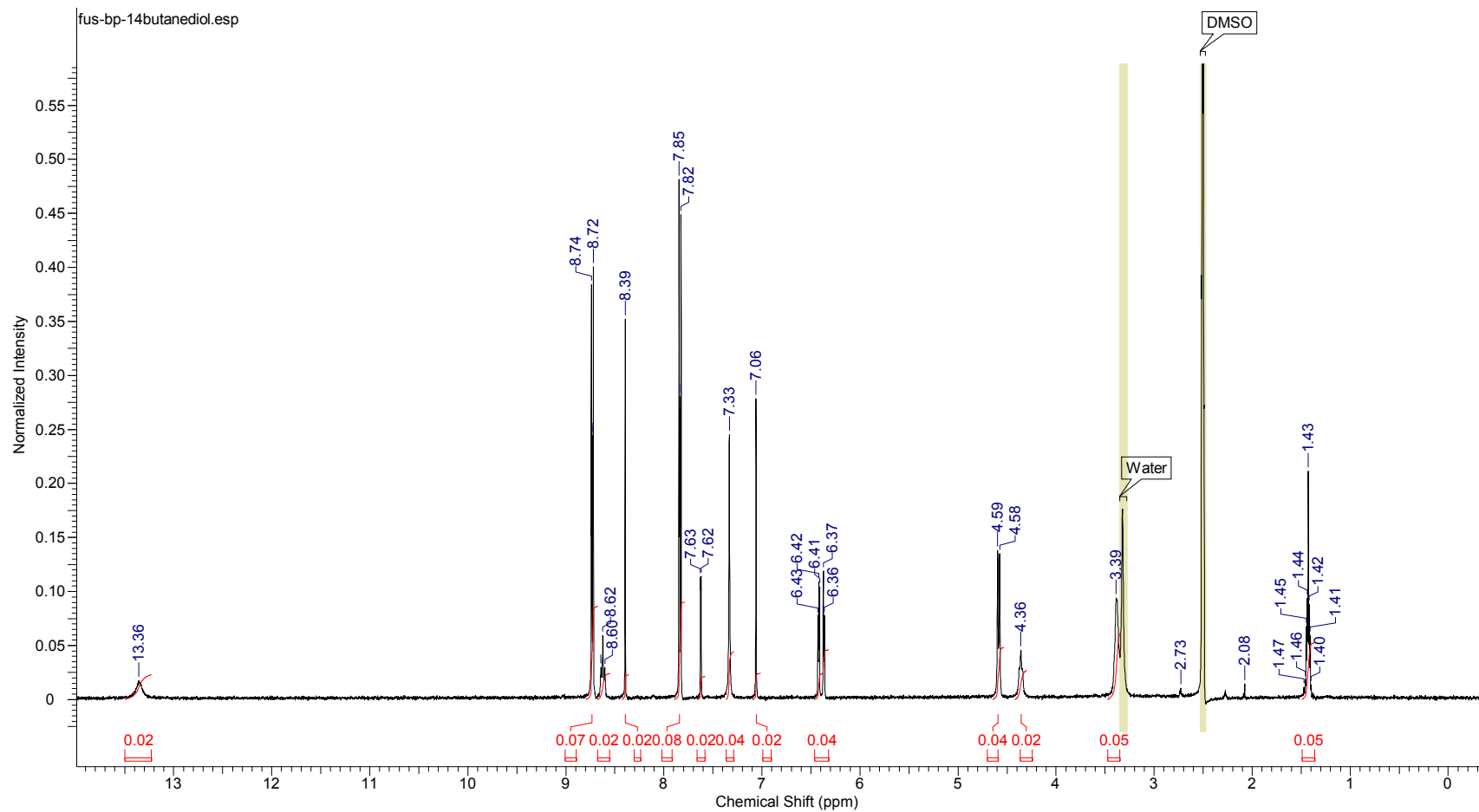
$^1\text{H-NMR}$  (300 MHz,  $\text{DMSO-d}_6$ ) of co-crystal (**8**) (furosemide-bipyridyl-ethylene glycol).

The  $^1\text{H-NMR}$  of co-crystal (**8**) recorded in  $\text{DMSO-d}_6$  is shown below. The  $^1\text{H-NMR}$  confirms that the bulk material of co-crystal (**8**) is a representative of the single crystal analysed. The integral values suggests that the co-crystal (**8**) contains furosemide, 4,4'-bipyridyl and the third component ethylene glycol in 1-1-0.5 composition.



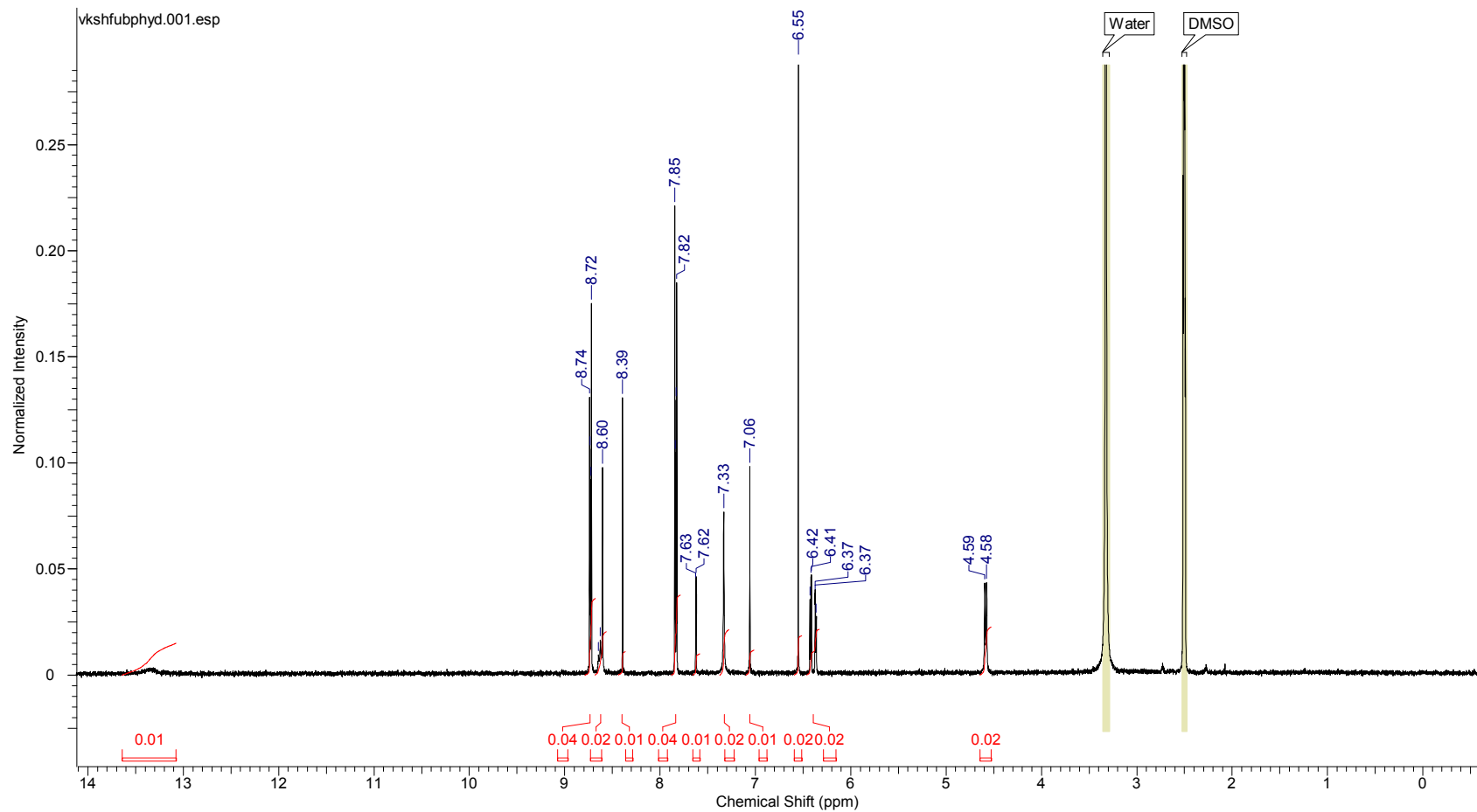
$^1\text{H-NMR}$  (300 MHz,  $\text{DMSO-d}_6$ ) of co-crystal (**9**) (furosemide-bipyridyl-1,4-butanediol).

The  $^1\text{H-NMR}$  of co-crystal (**9**) recorded in  $\text{DMSO-d}_6$  is shown below. The  $^1\text{H-NMR}$  confirms that the bulk material of co-crystal (**9**) is a representative of the single crystal analysed. The integral values suggests that the co-crystal (**9**) contains furosemide, 4,4'-bipyridyl and the third component 1,4-butanediol exists in 1-1-1 composition.



$^1\text{H-NMR}$  (300 MHz,  $\text{DMSO-d}_6$ ) of co-crystal (**10**) (furosemide-bipyridyl-hydroquinone).

The  $^1\text{H-NMR}$  of co-crystal (**10**) recorded in  $\text{DMSO-d}_6$  is shown below. The  $^1\text{H-NMR}$  confirms that the bulk material of co-crystal (**10**) is a representative of the single crystal analysed. The integral values suggests that the co-crystal (**10**) contains furosemide, 4,4'-bipyridyl and hydroquinone in 1-1-0.5 composition.



**8. Comparison of bulk powder X-ray diffraction data of ternary co-crystals (2), (3), (8) – (10) with respective single crystal simulated powder X-ray patterns.**

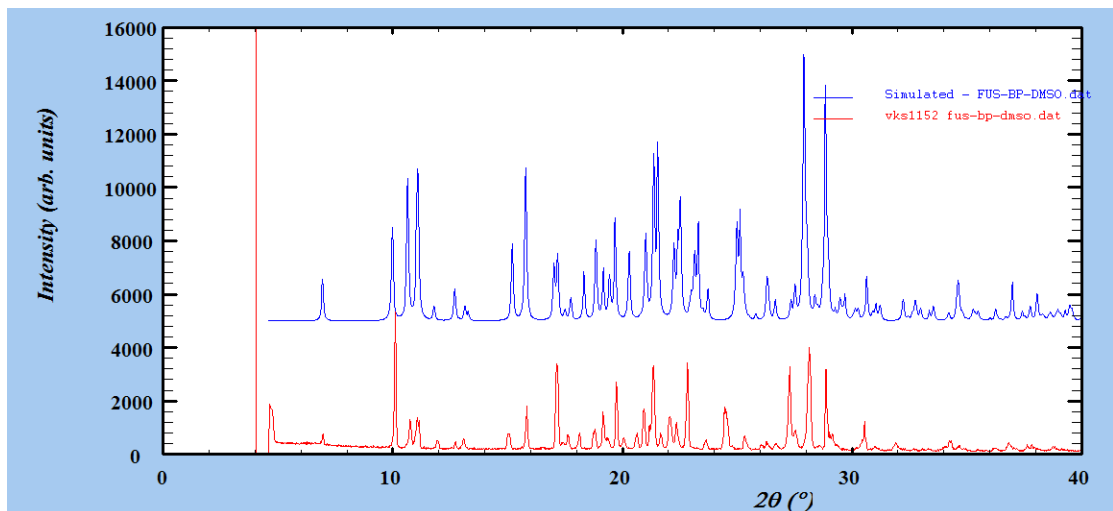


**Figure S35** Comparison plot of bulk powder X-ray diffraction data (red pattern) Vs single crystal simulated pattern (blue pattern) in co-crystal (2)

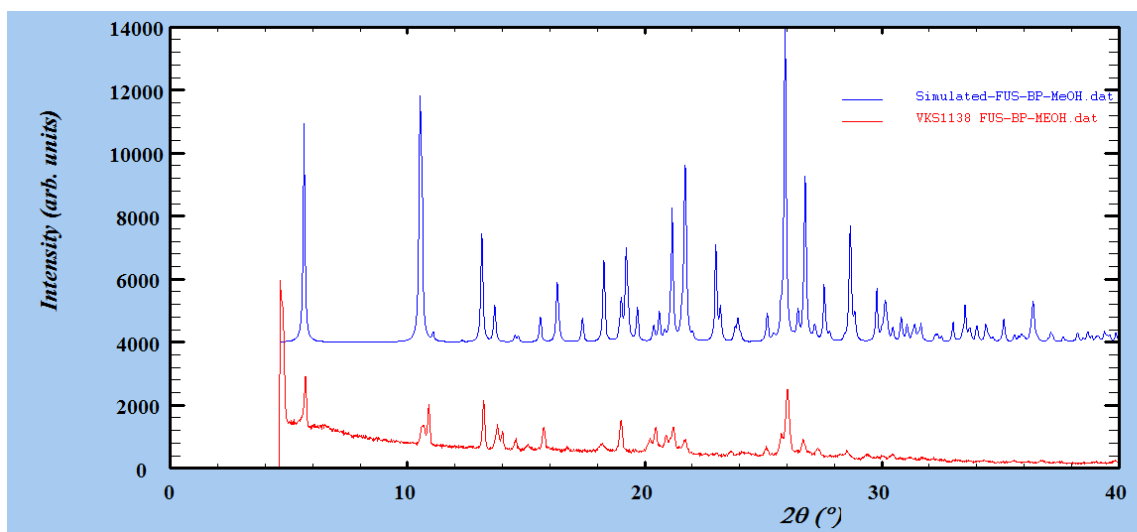


**Figure S36** Comparison plot of bulk powder X-ray diffraction data (red pattern) Vs single crystal simulated pattern (blue pattern) in co-crystal (3)

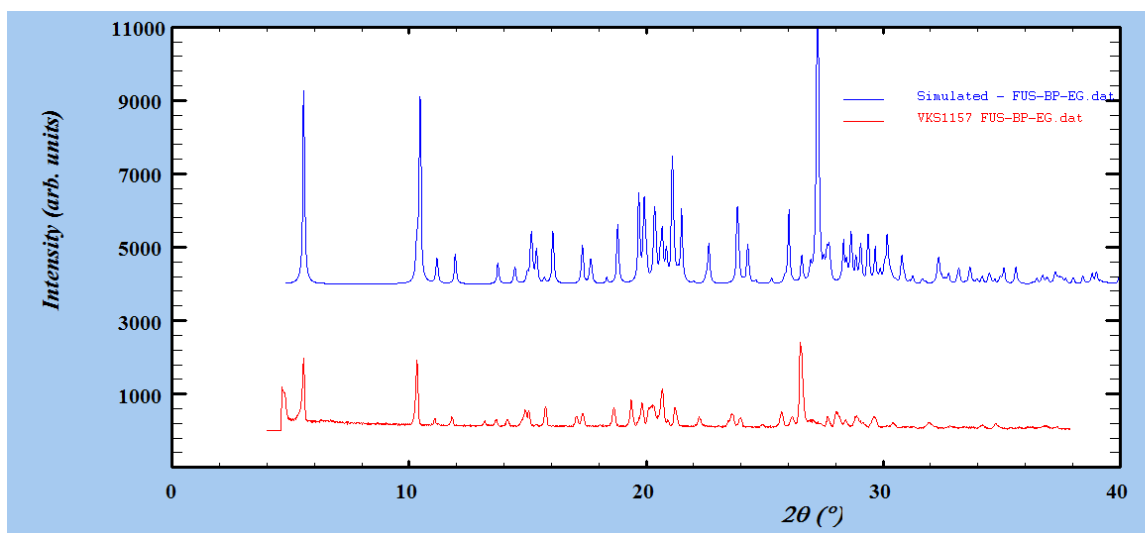


**Figure S37** Comparison plot of bulk powder X-ray diffraction data (red pattern) Vs single crystal simulated pattern (blue pattern) in co-crystal (8)

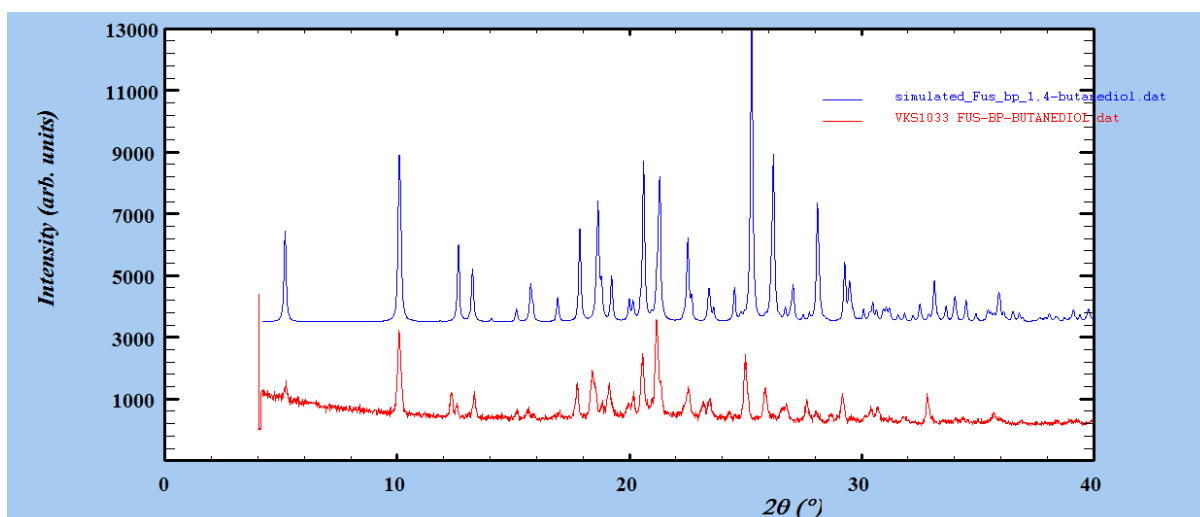


**Figure S38** Comparison plot of bulk powder X-ray diffraction data (red pattern) Vs single crystal simulated pattern (blue pattern) in co-crystal (9)

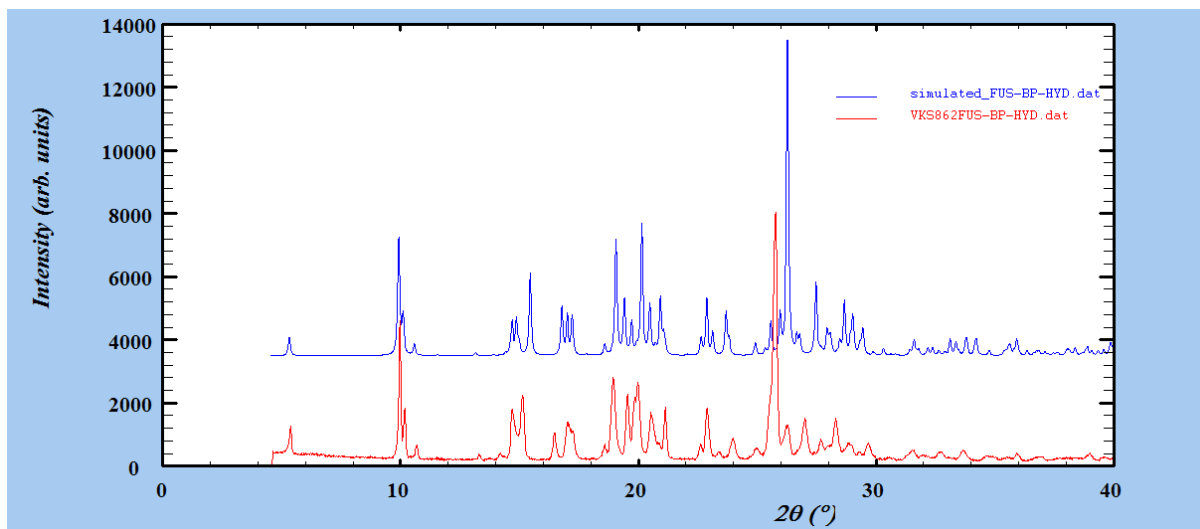


**Figure S39** Comparison plot of bulk powder X-ray diffraction data (red pattern) Vs single crystal simulated pattern (blue pattern) in co-crystal **(10)**